Lab on a Chip

CRITICAL REVIEW

View Article Online
View Journal | View Issue

Open Access Article. Published on 26 June 2023. Downloaded on 10/28/2025 9:16:10 PM.
This article is licensed under a Creative Commons Attribution 3.0 Unported Licence.

Check for updates

Cite this: *Lab Chip*, 2023, **23**, 3130

Integrated membranes within centrifugal microfluidic devices: a review

Killian C. O'Connell *[a] and James P. Landers[abc]

Centrifugal microfluidics has evolved into a sophisticated technology capable of enabling the exploration of fundamental questions in such fields as protein analysis, environmental monitoring, and live cell handling. These microdevices also hold unique potential for translating promising academic research into many real-world scenarios, with several products already available on the market. Yet, in order to fully realize this potentially transformative technology, there remains an outstanding need to incorporate simple to operate world-to-chip interfaces alongside the integration and automation of complex workflows. This requires cost-effective and versatile materials that are, ideally, already commercially available. Membranes not only meet these exigencies, they are also capable of enhancing the inherent advantages of microdevices when thoughtfully combined. This review provides an overview of the importance of these two technologies and the manifold benefits upon their unification. The fundamental principles governing fluid flow with centrifugal actuation, as well as within porous membranes, are briefly covered in addition to a comment on their relative advantages compared to classical microdevices and porous media. The major subtypes in membrane composition, preparation, and microfluidic integration strategies are next discussed in detail, along with their relativistic capabilities and drawbacks. This is followed by recent examples in the literature displaying the enormous versatility membranes have already demonstrated within microfluidic devices, highlighting recent centrifugal microdevices wherever possible. Finally, recommendations for areas where the incorporation of these materials still face challenges, as well as possible new avenues for exploration, are also provided.

Received 1st March 2023,
Accepted 16th June 2023

DOI: 10.1039/d3lc00175j

rsc.li/loc

Introduction

Microfluidics is the science and engineering of systems or processes that manipulate fluids in devices, or other flow-directing configurations, at submillimeter dimensions. This field lies at the intersection of numerous scientific disciplines, including analytical chemistry, molecular biology, materials science, and mechanical engineering, to name a few. This multidisciplinary approach is unsurprising given the origins of the field, which first evolved from the semiconductor industry (Fig. 1), as many of the same burgeoning technologies aimed at improving the production of silicon-based micromechanical systems (MEMS) in the 1960–70's were applied toward the creation of novel microdevices.[1,2] A major motivation for these innovative systems arose during the 1980's, with the rapid advancements in the field of genomics in pursuit of whole genome sequencing. There, the requirements for higher sensitivity, throughput, and resolution were best accommodated using microchip electrophoresis.[3] A second motivator stemmed from the exit of the cold war, as the United States Defence Advanced Research Projects Agency (DARPA) funded the development of field-deployable microfluidic sensors to counter the growing threat from chemical and biological weapons.[4] Amidst the convergence of these powerful technologies came rapid growth in the nascent field. In less than a decade, Terry *et al.* demonstrated the separation of gaseous hydrocarbons using a novel microscale gas chromatography system in what was later regarded as the first micro total analysis system (μTAS).[5] Prior to this, Anderson *et al.* developed the first rotating platform for clinical chemistry analysis,[6] which later served as the basis for a suite of new clinical analysis systems with applications in toxicology, immunology, haematology and beyond.[2] Both reported definitive performance enhancements due to the reduction in scale. Since then, many microfluidic devices capable of outperforming standard practices at the macroscale have been described, in both biochemical and chemical research.[7–9] Microfluidic devices have also achieved

[a] *Department of Chemistry, University of Virginia, Charlottesville, Virginia 22904, USA. E-mail: kco4yh@virginia.edu*
[b] *Mechanical and Aerospace Engineering, University of Virginia, Charlottesville, Virginia 22904, USA*
[c] *Department of Pathology, University of Virginia, Charlottesville, Virginia 22904, USA*

This journal is © The Royal Society of Chemistry 2023

Open Access Article. Published on 26 June 2023. Downloaded on 10/28/2025 9:16:10 PM.
This article is licensed under a Creative Commons Attribution 3.0 Unported Licence.

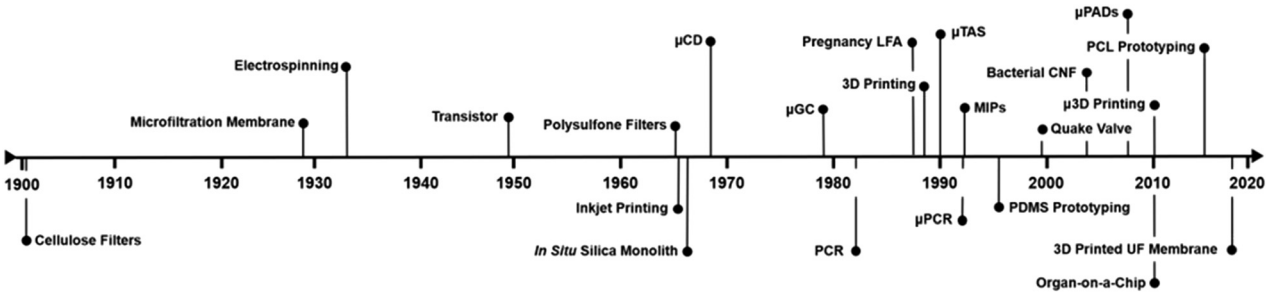

Fig. 1 Timeline highlighting the main advances within the field of microfluidics and membranes, along with several highly influential enabling technologies. Definitions for acronyms include: micro CD (μCD) otherwise known as centrifugal microfluidic devices, micro Gas Chromatography (μGC), Polymerase Chain Reaction (PCR), Lateral Flow Assay (LFA), micro Total Analysis Systems (μTAS) otherwise known as lab-on-a-chip, Molecularly Imprinted Polymers (MIPs), polydimethylsiloxane (PDMS), cellulose nanofibers (CNF), micro paper-based analytical devices (μPADs), print-cut-laminate (PCL), and ultrafiltration (UF).

novel functionalities that are unattainable at the macroscale, moving beyond straightforward performance enhancements.[10–14] Microscale fluid dynamics underlie the reasons behind these various advancements, as forces not normally relevant (*e.g.*, interfacial surface tension or van der Waals forces) begin to dominate[15] while heat and mass transfer are also more efficient.[16]

Pre-dating the rapid advancements in microscale engineering was the fascinating evolution of membrane technology (Fig. 1),[1,17] beginning in the 18th and 19th centuries. Initially, membranes were used exclusively for laboratory applications, and often consisted of sausage casings derived from animal intestines.[18] The invention of the first paper filter in 1908 by Melitta Bentz, for improving the taste and quality of brewed coffee, was among the first demonstrated uses of a membrane outside of the laboratory.[19] This was followed by the first microfiltration membrane, invented by the Nobel-prize winning chemist Richard Zsigmondy, which was produced commercially in 1927 by the pharmaceutical company Sartorius GmbH to test drinking water in Europe following the Second World War.[18] From that point on, membranes have been continually improved with regard to their composition and design (*e.g.*, pore size distribution, selectivity, lifetime, and production method) and have been adapted for use in many experimental as well as commercial applications.

Although there have been numerous comprehensive reviews in the literature separately covering advancements in membranes and microfluidic devices, there have been relatively few discussing the combination of these two technologies, and none focusing specifically on centrifugal microfluidics with integrated membranes. Perhaps this is unsurprising given centrifugal microfluidics still represents a burgeoning subtype within the field of microfluidics as a whole. Congruent to this may be the reliance on materials and practices which, although useful at the macroscale, do not readily lend themselves to microdevice assimilation without simultaneously increasing the cost and complexity of both the device and its associated hardware. Transitioning to a new class of materials, such as membranes, may not only advance centrifugal microdevice applicability, but also enable higher performance metrics. This is especially true for adaptive reagent storage strategies and the field of micro-chromatography. With nearly 1.5 million publications relating to membranes alone, there is clear access to highly customizable materials for advanced unit operations within microdevices, be they fundamentally structural or bio-chemical in nature. One possible roadblock in the recognition of their availability may be the numerous labels used to describe them throughout the literature. This review aims to highlight the importance of combining these technologies, with the hope of inspiring new research efforts.

Centrifugal microdevice fluid dynamics

The field of microfluidics research continues to pursue higher performative microdevices that offer decreased reagent and sample consumption, faster reaction kinetics, higher throughput, lower cost, spatial economy, and in some instances, portability. As a subset within the field of microfluidic "lab-on-a-chip" devices, centrifugal-reliant devices, also referred to as "lab-on-a-disc" (LoaD), offer several key advantages over more traditional microdevice designs. Namely, actuation of fluid flow over several orders of magnitude is achievable without the requirement for external fluidic connectors, necessitating solely a compact motor in place of syringe pumps. This enormously reduces the complexity and time required for user-interaction, while also limiting the cost and enabling portative capabilities. Moreover, as fluidic processing steps require only simple changes in the applied spin frequency, a reduction in dead volume as well as streamlining of complex assay protocols is achievable. Interfacing control of the entire system with a laptop or other handheld computer is also facile. A wide array of fluidic operator functions for more precise manipulation of fluids, including mixing,[20,21] metering,[22,23] separation (both physical and chemical),[24,25] and valving (both passive and active)[26,27] have been extensively enumerated. Finally, even multi-step assays can be performed in a high-throughput

Open Access Article. Published on 26 June 2023. Downloaded on 10/28/2025 9:16:10 PM.
This article is licensed under a Creative Commons Attribution 3.0 Unported Licence.

manner, by copying the initial architecture across the device surface and running all 'domains' simultaneously.

There are several distinct forces† responsible for governing microscale fluidic manipulation, all of which have been thoroughly covered by several excellent reviews.[2,28–30] There are also several flow control mechanisms, unique to centrifugal microfluidics, that have been mathematically enumerated including 'flow switching'[31] and the actuation of siphon valves independent of spontaneous capillary flow.[32] Unlike other methods of fluid actuation, centrifugally pumped liquids are relatively insensitive to the physicochemical properties of the fluid (*i.e.*, ionic strength, flow rate, and pH).[2,28,33,34] Instead, centrifugal flow depends upon the rotational frequency applied, the location of the fluid plug, the properties of the fluid that factor into its inertia, such as viscosity (μ), and the physical characteristics of the microchannel geometry. This is summarized in Fig. 2,[28] where the relationship between these variables to the average fluid velocity ($\bar{v}$) within a channel are defined in eqn (1) below,

$$\bar{v} = \frac{D_h{}^2 \rho \omega^2 \bar{r} \Delta r}{32 \mu L} \tag{1}$$

Here, L represents the length of the liquid in the microchannel. The magnitude of $\bar{v}$ reaches a local maximum in the center of the channel as denoted by a parabolic flow profile. D_h represents the hydraulic diameter of the channel and can be calculated from $4A/P$, where A is the cross-sectional area of the channel and P the wetted perimeter. From this, the volumetric flow rate (Q) can be defined as $Q = \bar{v} \times A$, with $\bar{v}$ derived from the previous formula. Prediction and control over Q can be a key aspect in proper microdevice functioning as well as assay performance.[35–37] Notably, variations on this equation‡ can account for the specific cross-sectional geometry of individual channel structures.[38]

Centrifugal flow within porous substrates

Unlike the initial attempts at microdevice fabrication in the 1980–90's, glass and silicon have been largely superseded by plastics. There are numerous reasons for this transition, with arguably the most important being the reduced cost and complexity for rapid prototyping.[24,39–41] This transition also improves the amenability of these devices for industrial manufacturing processes. However, more recently, metal and glass have returned for the construction of more specialized device components, oftentimes due to their intrinsically higher chemical and thermal stability.[4] One example of an integrated component that is usually, though not always, composed of a material distinct from the bulk of the microdevice are microscale membranes. Membranes are functional materials composed of interstitial voids capable of partitioning selective constituents within a fluid. An important distinction between porous membrane materials and a generalized porous substrate is the interconnected nature of the interstitial voids, permitting fluidic passage, as opposed to a porous substrate that may contain internal voids but no channel network permitting flow. For this unique class of porous materials both the physical structure, or existing chemical surface, can be exploited or further functionalized to achieve new performance metrics. The integration and value of these porous membranes for centrifugal microfluidics will be the primary focus within the following review. Finally, for the purposes of this discussion, a distinction will be made between "packed bed columns" and "porous membranes". Although similar in many ways, the materials, fabrication, microfluidic integration, and methods for use between these two substrates differ substantially. The definition of a membrane will therefore include the interconnection of the physical substrate, such as in monoliths, as opposed to discrete particles.

A distinguishing feature of porous media is the three-dimensional interconnected network of capillary channels, often with nonuniform sizes and shapes[42] (Fig. 3).[43–54] Despite the inherent complexities of these substrates, some characteristics of fluidic movement can be approximated by separate formulae. For example, the flow rate (Q_P) within a porous structure is characterized by Darcy's law, which accounts for the hydraulic conductivity of the substrate. This

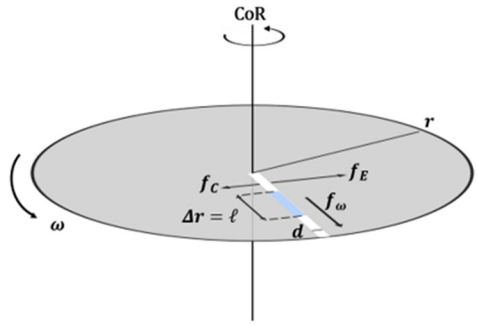

Fig. 2 Forces acting on a fluid plug propelled within a centrifugal disc. The angular frequency (ω) of the disc determines the magnitude of the centrifugal (f_ω), Coriolis (f_C), and Euler (f_E) forces according to opposing vectors. The liquid plug, with a diameter (d) and absolute length ($l = \Delta r$), is shown at an average radial distance ($\bar{r}$) from the center of rotation (adapted from ref. 28).

† Each of the 'forces' which are considered influential for governing fluidic behavior in centrifugal microfluidic devices (*e.g.*, the centrifugal force, Coriolis force, and Euler force) are considered to be pseudo or inertial forces. Inertial forces do not arise from the physical interaction between two objects and are instead explanatory artefacts arising from a description of motion using a non-inertial frame of reference. According to Newton's second law of motion, in the form $F = m \times a$, pseudo forces are always proportional to an object's mass. In this instance, the mass refers to that of a liquid plug.[325]

‡ Most common are rectangular cross-sectional channels, where the height (h) ≪ width (w). The volumetric flow rate in this instance can be calculated as (eqn (1.1)),[38]

$$Q = \frac{h^3 w (\Delta p_c + \Delta p_h)}{12 \eta L}\left[1 - 0.63\frac{h}{w}\right] \tag{1.1}$$

Open Access Article. Published on 26 June 2023. Downloaded on 10/28/2025 9:16:10 PM.
This article is licensed under a Creative Commons Attribution 3.0 Unported Licence.

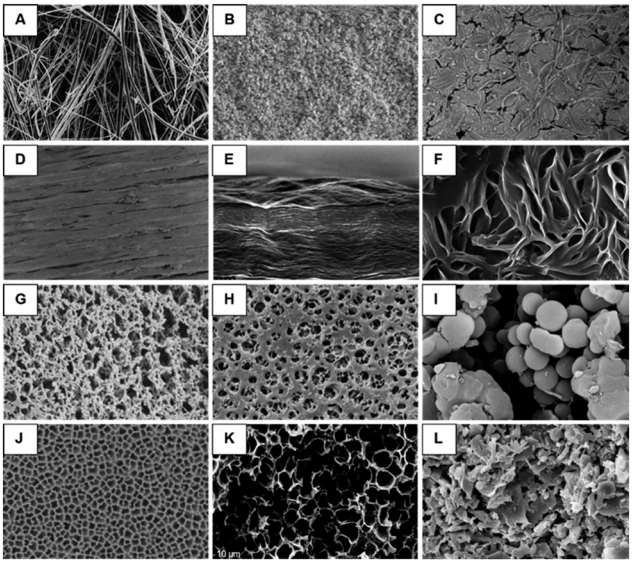

Fig. 3 SEM micrograph of membranes composed of A. binder-free quartz microfiber with 1 μm pores (adapted from ref. 43). B. High density (HD) Empore™ disk with 10–12 μm functionalized silica beads enmeshed within PTFE fibrils (adapted from ref. 44). C. Sol–gel PEG coated cellulose fabric surface at 100× magnification (adapted from ref. 45). D. 1.75 mm LAY-FELT 3D printing filament after dissolution of water soluble PVA at 65× magnification (adapted from ref. 46). E. Edge view of graphene oxide (GO) membrane showing lamellar texture (adapted from ref. 47). F. Bacterial cellulose paper produced by *Gluconacetobacter xylinus* at 15 000× magnification (adapted ref. 48). G. Advantec MFS nylon membrane filter with 0.1 μm pores (adapted from ref. 49). H. Sartorius cellulose acetate membrane filter with 0.1 μm pores (adapted from ref. 50). I. 0.9–1.2 μm diameter molecularly imprinted polymer (MIP) beads bound to an ion-conductive membrane (adapted from ref. 51). J. 100 nm Anopore™ AAO membrane (adapted from ref. 52). K. Carbon monolith magnified 3700× (adapted from ref. 53) and L. cross section of a mullite tubular ceramic membrane (adapted from ref. 54).

measured value for a particular media is called the specific permeability (k),§ and is independent of fluid properties and flow mechanisms, but uniquely determined by pore structure. According to eqn (2),[55]

$$Q_P = \frac{-kA}{\mu} \times \frac{(p_2 - p_1)}{L} \tag{2}$$

The flow rate through a porous substrate is therefore also affected by the cross-sectional area of the microstructure as well as the pressure drop ($\Delta P = p_2 - p_1$), where ΔP is the difference in total pressure between two points in a channel. These values can be specified and modulated for an integrated membrane within a microfluidic channel. To inform this modulation ΔP can be further defined as,[56]

§ The general term for permeability is affected both by the properties of the permeating fluid as well as the mechanism of permeation. Specific permeability refers to the measure of contribution of the porous media to fluidic conductivity and is independent of both fluid properties and flow mechanisms. The phrase permeability used throughout this text will refer to specific permeability.

$$\Delta P = \frac{8\pi\mu L Q}{A^2} \tag{3}$$

According to eqn (3) the pressure drop is largely a function of channel geometry.

As will be further discussed in subsequent sections, edge sealing around integrated membranes can present unique challenges for microdevice fabrication. An escalation in the pressure drop, either through the inclusion of a resistance channel[35] or a larger channel cross-sectional area or membrane pore size, or are all common strategies to help avoid liquid bypass. However, depending upon microdevice construction, it is important to note that effective cross-sectional areas can be increased according to separate mechanisms: concomitant channel and membrane widening for instances of linear flow, or solely membrane enlargement for orthogonal flow (*e.g.*, a liquid must either drop down or rise through a membrane to access channels located above and below the porous substrate). In the latter scenario, membrane efficiency may become negatively impacted specifically during centrifugal flow actuation. One strategy to avoid this phenomenon involves liquid priming.[57] Pressure gradients in the channel immediately above a porous substrate will induce a nonuniform pressure drop across the membrane surface (Fig. 4A).[58] This is due to the increased pressure experienced by the edge of the membrane closest to the outer boundary of the disc, which is able to overcome the capillary resistance of the membrane.[59] This can result in inefficient use of the membrane's total capacity, as flow is solely induced across a small fraction of the total accessible surface. However, with the inclusion of a priming liquid (Fig. 4A), the pressure gradient above and below the membrane may be balanced for uniform flow through the entirety of the integrated membrane.[58,60] Consideration and appropriate accommodation of such centrifugal fluid dynamics behaviour can significantly impact membrane, and therefore microdevice, performance.

Conversely, by taking advantage of this phenomenon, membranes may also act as configurable gates with the inclusion of a capillary-stabilized liquid retained within the interstitial voids (Fig. 4B).[59] The gating threshold (*i.e.*, the pressure needed to open the membrane pores and allow fluidic bypass), wherein the retained liquid remains capable of reversibly reconfiguring in place, may be tuned over a wide range of applied pressures. This ultimately allows for differential response profiles across a variety of liquids and gasses, as well as sustained anti-fouling capabilities. This gating threshold (ΔP_g) is proportional to the flow rate and viscosity of the incoming fluid as well as the membrane permeability (eqn (4)),[59]

$$k = \frac{\Phi}{32\tau^2} \int_{\frac{2\gamma}{\Delta P_G}}^{\infty} \frac{X^2}{\sigma\sqrt{2\pi}} e^{\frac{(X-d)^2}{2\sigma^2}} dX \tag{4}$$

where Φ is the membrane porosity, τ is the membrane tortuosity, d the mean pore size, and σ the standard deviation around d (assuming a normal distribution). In this case, γ

Open Access Article. Published on 26 June 2023. Downloaded on 10/28/2025 9:16:10 PM.
This article is licensed under a Creative Commons Attribution 3.0 Unported Licence.

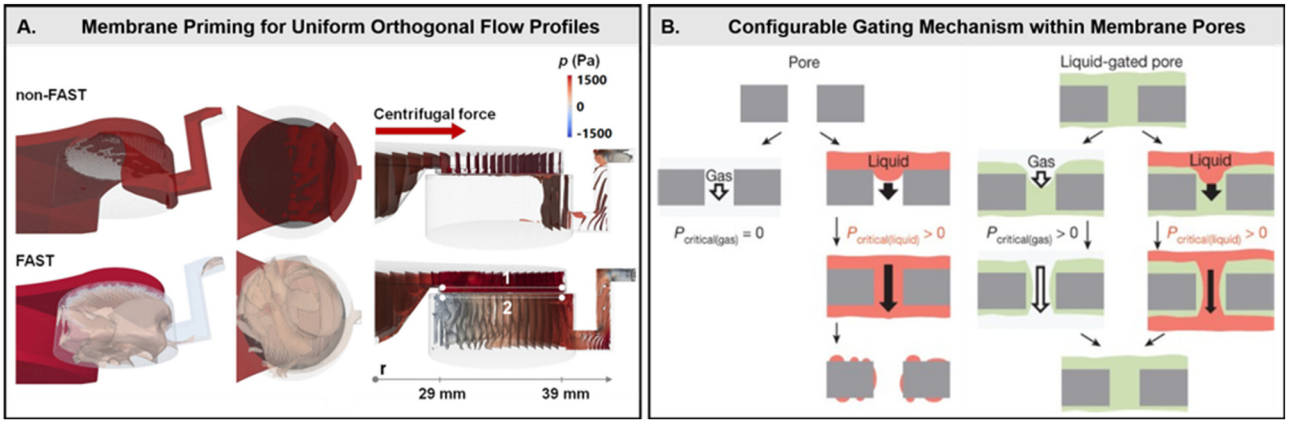

Fig. 4 Unique flow behavior through liquid-primed membranes. A. Numerical analysis illustrating pressure contours induced *via* centrifugal force in a non-fluid assisted separation technology (FAST) (top) and FAST (bottom) mode. A nonuniform pressure drop across an embedded membrane is observable in the non-FAST mode, with only a small percentage of the membrane in use. In contrast, after liquid priming of the membrane a uniform pressure drop is achieved, significantly improving membrane efficiency (adapted from ref. 58). B. Difference between gas *versus* liquid (red) penetration (left) through a nano- or micro-scale pore. Gas transport occurs freely in contrast to the minimum threshold required for liquid penetration. A retained liquid (green) within a liquid-gated pore (right) prevents free gas exchange, instead requiring a unique pressure threshold for both incoming liquids (red) and gasses. The gating liquid is capable of reconfiguring, and enables tunable control over multiphase transport (adapted from ref. 59).

refers to the surface tension between the incoming fluid and the liquid retained within the membrane. This system enables fast and consistent control over multiphase flow through a porous membrane, contained within a microfluidic channel network, *via* simple adjustments in applied pressure. As described earlier, centrifugal microfluidic devices are highly amenable to automation of this fluidic control mechanism.

Membrane materials & functionalization strategies

A quick search with the keywords 'membranes' and 'microfluidic devices' returns over 7400 results, according to Clarivate Analytics Web of Science (Fig. 5A). This number is all the more striking given that many integrated membranes are not coined as such within a given article, and are instead described according to structure or function (*e.g.*, filter, monolith, sieve, porous support, array, or film).[61] As evidenced by the rise in publications highlighting their use (Fig. 5B), as well as several historical and recent review articles (*e.g.*, Jong *et al.*,[61] Chen *et al.*,[62] and Yuan *et al.*[63]), compelling reasons for incorporating these immensely versatile materials within microdevices clearly exist. The increasing selection of these functional materials may be partially attributed to the vast possibilities in membrane composition; an enormous number of both organic and inorganic substrates are available for a variety of applications. Despite this, a search for membranes in centrifugal microfluidic devices returns a paltry 62 results, revealing an underutilized pairing within the field. Consequently, although the following review will discuss the use of membranes in all types of microfluidic devices, centrifugal microdevices will be highlighted wherever

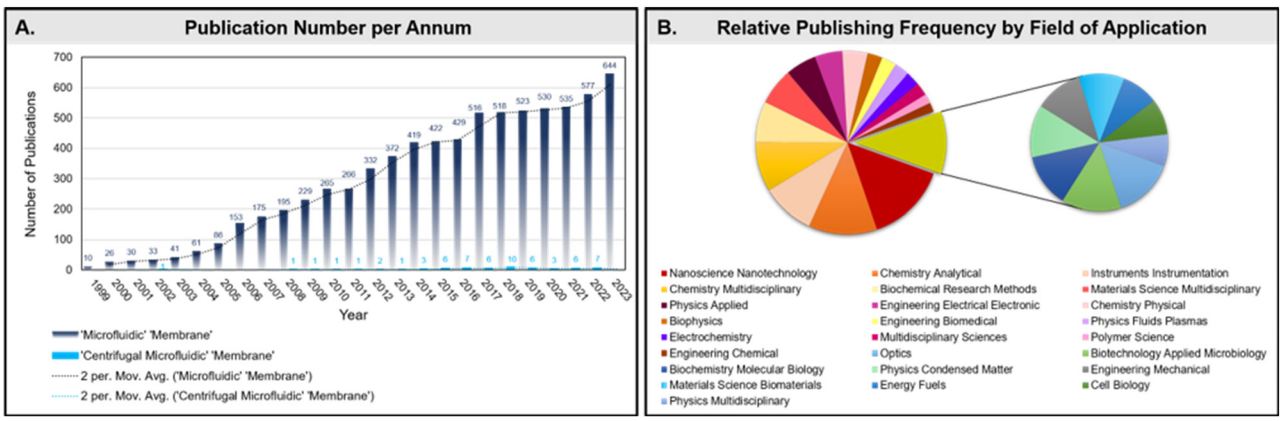

Fig. 5 Clarivate Analytics 'Web of Science' analysis of results. A. Total number of publications per year, from 1999–2023, for membranes in microfluidic devices. B. Pie chart of relative frequency of publications according to research discipline.

Open Access Article. Published on 26 June 2023. Downloaded on 10/28/2025 9:16:10 PM.
This article is licensed under a Creative Commons Attribution 3.0 Unported Licence.

possible. Due to the enormous variety in material type and application, this review is by no means exhaustive. In an attempt to narrow the focus of the following overview, only solid-state membranes will be discussed, although it is worth noting that other specialized membrane phases (*e.g.*, liquid) have also been demonstrated within microfluidic devices as highly selective partitioners.[64] Among solid-state membranes, only those whose constitution differs from the microdevice bulk material, or whose fabrication procedure represents a novel extension of the microdevice assembly process, will be included. Likewise, microdevices that make use of the pre-existing substrate, either as microfluidic paper or cloth-based analytical devices (μPADs or μCADs) or composed solely of poly(dimethyl sulfoxide) (PDMS),[65–67] for functioning as a membrane will not be included.[61,68] Finally, biological membranes (derived *in vivo*) will also be excluded from this discussion due to their markedly unique integration strategies and usages.[69–71] However, this exclusion does not extend to synthetically processed membranes (derived *in vitro*) that have been additionally functionalized with biological material, or are classified as "biomimetic", nor to the biopolymer cellulose derivatives.

Silicon & metals

For applications requiring either extremely high thermal or chemical resistance, high porosity, low tortuosity, electrical conductivity, complex nano-scale features, or exceptionally narrow pore size distributions, anodized membranes are the predominant choice. This class of membrane is made of either inorganic silicon or aluminium, with the latter element prevailing as the substrate of choice for several reasons,[72] the most important of which relates directly to the preparation of the passivated surface.[72] The process of electrochemical passivation increases the natural surface oxide layer, lending these membranes their highly resistance characteristics. However, anodization of silicon requires hydrofluoric acid, in comparison to the relatively benign oxalic acid for aluminum. Additionally, the aspect ratio (pore diameter to membrane thickness) is far more constrained for silicon; leading to brittle, wafer-thin membranes that are difficult to handle. In contrast, anodic aluminum oxide (AAO) membranes can achieve high aspect ratios with tuneable pore sizes (4–200 nm) and array spacing.[73] The final attributes which make AAO membranes particularly attractive for microfluidic applications are their optical transparency and non-cytotoxicity.[74] Furthermore, the ability to generate complex nano-scale features, in combination with their lack of cytotoxicity, offers particular potential in the field of cell biology, where single-cell and exosome analysis continues to increase in importance (Fig. 6A).[75] AAO surfaces can also be functionalized to tune their selectivity for multi analytes simultaneously (Fig. 6B).[76] Similarly, the optoelectronic properties offer great potential in the realm of diagnostics development,[77] another rapidly growing sector within microfluidics. Commercial preparation of AAO surfaces has been a standard practice within industry for several decades, rendering the equipment required for custom fabrication readily available. Yet it should also be noted that both AAO

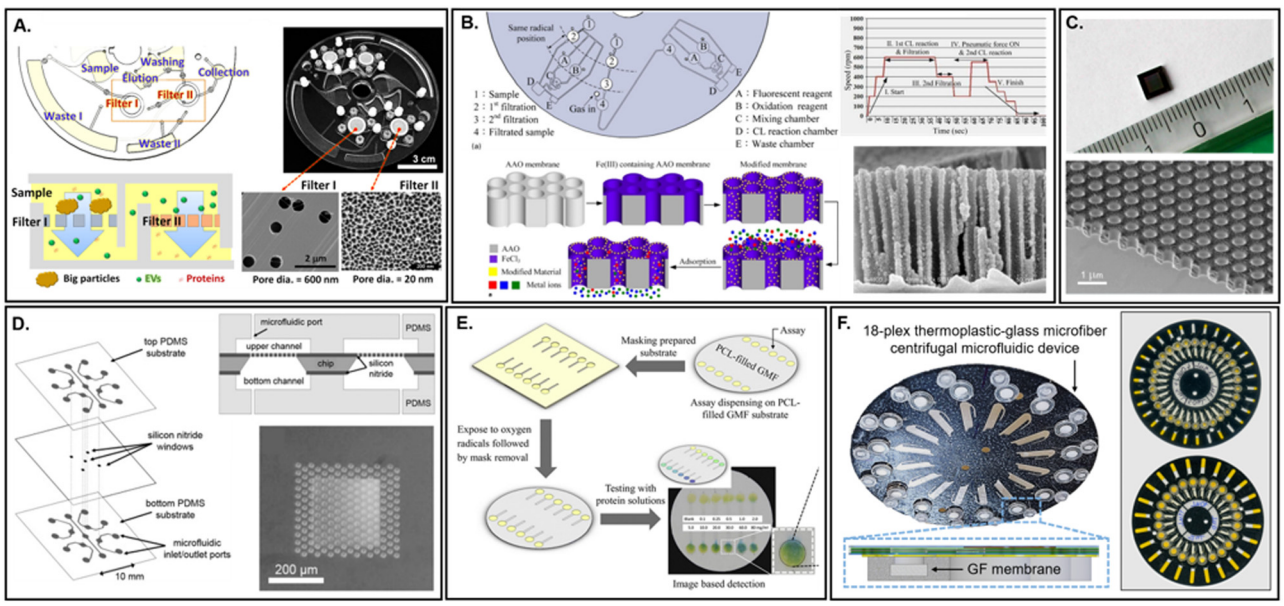

Fig. 6 Membranes composed of inorganic metal, silicon, and silicates. A. Monolithic AAO membrane integrated within a closed microfluidic device. Chip dimensions are 6.5 × 9 × 1.3 mm (adapted from ref. 75). B. Multi-modified AAO nanoporous membranes for heavy metal detection (adapted from ref. 76). C. Silicon nitride as lipid membrane holder for protein crystallography (adapted from ref. 90). D. Self-supporting silica thin (100–200 μm) film membrane as a gateable interconnect for microfluidic devices (adapted from ref. 78). E. Superhydrophilic polycaprolactone (PCL) filled glass microfiber membranes for total protein determination (adapted from ref. 85). F. Unmodified glass microfiber (GF) membranes for wet acid microwave assisted extraction (MAE) of heavy metals (adapted from ref. 89).

Open Access Article. Published on 26 June 2023. Downloaded on 10/28/2025 9:16:10 PM.
This article is licensed under a Creative Commons Attribution 3.0 Unported Licence.

and silicon oxide membranes are available commercially from vendors such as GE Whatman and Sterlitech.

Additional metal and silicon membrane materials include noble metals (*e.g.*, palladium, titanium, platinum, or silver) and silicon nitride. As these materials are expensive to either fabricate or purchase commercially, their use remains limited for specialized applications. Silicon nitride, a non-oxide ceramic, is non-transparent, prohibiting any desired imaging procedures in the visible spectrum. However, the material does possess the relatively unique characteristic of low background scattering and high X-ray (Fig. 6D)[78] and microwave[79] transmissibility. Noble metal membranes may either be incorporated as thin films[80] or as nanoparticles sputtered onto ceramic nanofibers.[81] Noble metal membrane compositions are primarily sought for their superior catalytic behaviour and have thus been largely applied toward reactions involving hydrogen, although their use for augmenting surface enhanced vibrational spectroscopy has filled a critical niche within microfluidics.[82] One downside to the fabrication and implementation of metallic membranes in particular, beyond the up-front investment required, is their poor ability to bind to polymers, which can limit or otherwise complicate microdevice integration.[83] Furthermore, their reactive surfaces can compromise structural integrity or interfere with assay performance.[84]

Silicates

Silicates are an especially important class of inorganic, microwave and ultraviolet (UV)-transparent, biocompatible membrane substrate. The production, functionalization, and use of these materials has been widely employed in industry for decades. The abundance of precursor substrates, in addition to specialized products, makes this material highly accessible and in many cases affordable. Modifications to achieve the requisite physicochemical surface properties can be tailored to specific applications. For example, although normally hydrophilic, silicates can be permanently altered to become superhydrophilic (Fig. 6E),[85] hydrophobic or even superhydrophobic.[86] Methods for advanced surface functionalization are also readily available, with a recent example harnessing a chitooligosaccharide modified surface for aqueous nucleic acid purification.[87] Silicates can additionally be prepared in a variety of form factors,[88] including nano- or microfibers (Fig. 6F),[89] thin films (Fig. 6C),[90,91] nanotubes,[92] or as embedded colloids.[44,93] Although membrane pore size distribution is typically low, this will vary depending upon the microphysical structure and fabrication method used. Compared with most polymeric networks, silicates offer superior chemical and thermal resistance coupled with a lower potential for contamination in analytical procedures. For elemental analysis of solid samples, which can require intensive extraction procedures,[94] the low risk for contamination is crucial. An exception to this attribute includes minimal hydrothermal resistance to the presence of water vapor at very high (100–600 °C) temperatures.[95] Yet apart from micro Gas Chromatography (μGC),[96] this circumstance rarely limits the selection of silicate substrates, as these temperatures are not often employed in conjunction with microfluidic devices. Borosilicates in particular are even capable of withstanding standard autoclaving procedures. Finally, silica is also not resistant to strong alkaline solutions, concentrated phosphoric acid, or hydrofluoric acid.

Like polymers, silicates can be prepared as membranes either prior to device integration or *in situ*. Surface activation, through oxidation of surface silanol moieties, makes direct bonding and grafting to a variety of synthetic or biopolymers possible. Notably, silicate membrane fibers will not absorb protic or nonprotic solvents, thereby reducing their effective pore size over time due to swelling. The drawbacks for employing this material include its opacity in the visible region (when micro-structured) and a high propensity for surface fouling with biomolecules without pre-treatment. Although this last property has also been extensively leveraged as an efficient capture mechanism for both nucleic acids[97,98] and proteins.[99] Among the various silicates available, borosilicate is used most frequently, although fused silica and zeolites (*i.e.*, aluminosilica) are also reported.[84,100]

Carbon & graphene oxide

Activated carbon offers a unique suite of characteristics as a membrane material. Analogous to silicon, carbon is electrically conductive and generally hydrophobic, enabling the performance of electrochemical reactions in conjunction with molecular separation on the basis of size or chemical functionality. These conductive membranes offer a mechanism for microfluidic electrophoresis, electroosmosis, or electrochemical redox, in addition to harnessing electrostatic repulsion as a membrane fouling mitigation strategy.[101] However, electrochemical capabilities can be negatively impacted by the ionic strength of the aqueous solution passing through the membrane. Akin to polymers,[102] carbon can be prepared in the form of nanofibers[103,104] or through *in situ* generation of sol–gel monoliths[53,105] and hydrogel composites.[106,107] This renders the substrate highly structurally diverse.[108] Furthermore, carbon membranes exhibit high chemical, thermal, and mechanical stability (although important exceptions do exist), coupled to widely available bio- or enviro-sourced precursors (*e.g.*, cellulose or graphite) which maintains a much lower cost point compared to other inorganic substrates.[109] As yet, carbon-based membranes remain underutilized within the field of centrifugal microfluidics. This can likely be ascribed, in part, to the limited availability of commercial membranes.

Among the many possible physicochemical forms of carbon-based membranes, one material in particular provides comprehensive insight into the possibilities and challenges

 This journal is © The Royal Society of Chemistry 2023

Open Access Article. Published on 26 June 2023. Downloaded on 10/28/2025 9:16:10 PM.
This article is licensed under a Creative Commons Attribution 3.0 Unported Licence.

of the material as a whole. Graphene oxide (GO) is composed of an ~1 nm thick plane of covalently linked, oxygen-derivatized carbon. The highly disparate height (nanometer) and width (nano- to micrometer) of these layers bridges the conventional length scales of both chemistry and materials science.[110,111] Each layer exhibits amphiphilic qualities, with the basal surface consisting of partially oxidized aromatic rings, in contrast to the layer edges which are composed of carboxylic acid groups.[112] This amphiphilic character allows for not only multi-layer lamellar assembly, through interfacial manipulation,[113] but also phase selective flow control[114] and liquid gating.[115] Similar to cellulose polymers, this abundance of available chemical moieties renders GO surfaces highly versatile. Yet unlike graphene, which is composed of a monomolecular layer of aromatic carbon rings, GO is electrically insulating. Restoration of electrical conductivity can be achieved through thermal, chemical, dielectric, or photo-reduction, resulting in what is known as reduced GO (rGO).[116,117] However, although the electrical conductivity of rGO is considered sufficient for many applications, it does not achieve the same level of efficiency as pristine graphene.[112] Though not commercially available, the straightforward synthesis of GO membranes from inexpensive graphite powders has been described extensively within the literature,[118–121] with a vast array of different techniques available for tuning interlayer spacing and membrane stability. Notably, insufficient removal of potassium salt impurities has been found to significantly reduce thermal stability,[122] necessitating extensive wash procedures during membrane fabrication.

Both GO and rGO offer many desirable qualities as a membrane material, including biocompatibility and resistance to compression. Nevertheless, several potential downsides to this membrane type exist. Both GO and rGO are opaque, with disordered pore morphology, and a propensity for protein adsorption due to the same electrostatic interactions which enable self-assembly.[123] These materials have also historically been difficult to integrate within microfluidic devices as the graphitic surface does not bind readily to polymers,[114] among other potential microdevice materials. However, GO or rGO composites may offer an alternative means for microfluidic integration beyond a reliance on adhesives,[47] in addition to imparting novel characteristics such as enhanced tensile strength.[115] Finally, although lamellar GO flakes remain heavily favored as a membrane substrate, alternative porous structural formats offer novel avenues for microdevice applications, including the use of GO microfibers[117] as a culturing scaffold for organ-on-a-disc,[124] asymmetric bilayers for integrated power generation,[125,126] or hydrogels for sensors[127] and catalysis.[128] These new structural forms would also offer new challenges and opportunities with regard to microfluidic integration strategies.

Synthetic polymers

Synthetic polymeric membranes represent a vast category of possible materials, with subtypes usually classified as elastomers, thermoplastics, or thermosets.[129] The physicochemical properties, functionalization strategies, and fabrication methods are equally considerable. Due to the size of this category, only two polymer membrane types will be featured: poly(dimethylsiloxane) (PDMS) and molecularly imprinted polymers (MIP), due to their historically extensive or growing use within the field of microfluidics. However, additional porous materials, that are infrequently employed at present, will also be briefly highlighted. Importantly, these ancillary materials are commercially available and represent critical opportunities for use in microfluidic devices. A final comment on an emerging class of hybrid polymeric membranes, not yet commercially available nor employed within microfluidic devices to the best of our knowledge, is also included.

There are several properties of polymers that extend across nearly all subtypes and can be cautiously generalized. First, the price investment for these materials is typically low. This is especially true when paired with the cost of fabrication and compared on a per-membrane basis with silicon, metallic, and even some silicate membranes. Only cellulose membranes are able to compete in this category. Second, relative to other inorganic membranes, polymer networks do not offer high thermal resistance thresholds (<300 °C) nor are they as chemically resistant.[84] However, some chemically inert polymers (*e.g.*, fluorinated polymers, polyether ether ketone, *etc.*) are able to resist highly oxidizing or reducing reagents (*e.g.*, hydrofluoric or phosphoric acid) that are incompatible with either metals or silicates, especially at elevated temperatures. This resistance is unique among the materials discussed and can be especially useful when avoidance of nonspecific binding or corrosion is desired. Third, the available form factors for polymers are unsurprisingly extensive, although feature resolution is highly dependent on the individual polymer (or polymer composite) and fabrication method employed.[73] Incidentally, there exist polymer resins from each of the major subtypes that are amenable to 3D printing. However, the total number of resins available for this fabrication procedure still represents a small fraction of the entire polymer division.[130] Last, although polymers are normally considered distinctly suited for translation to commercial manufacturing, micro-scale membranes are a relatively new structural capability for these materials. Despite the rapid increase in commercial R&D to optimize performance and durability, control over preparation procedures remains problematic. Therefore, relatively few commercial polymeric membranes are available. Notable exceptions include fibrous polytetrafluoroethylene (PTFE) mats, particle loaded membranes (PLMs), or polyethylene/polycarbonate track-etched thin films (Fig. 7A).[131–133]

Open Access Article. Published on 26 June 2023. Downloaded on 10/28/2025 9:16:10 PM.
This article is licensed under a Creative Commons Attribution 3.0 Unported Licence.

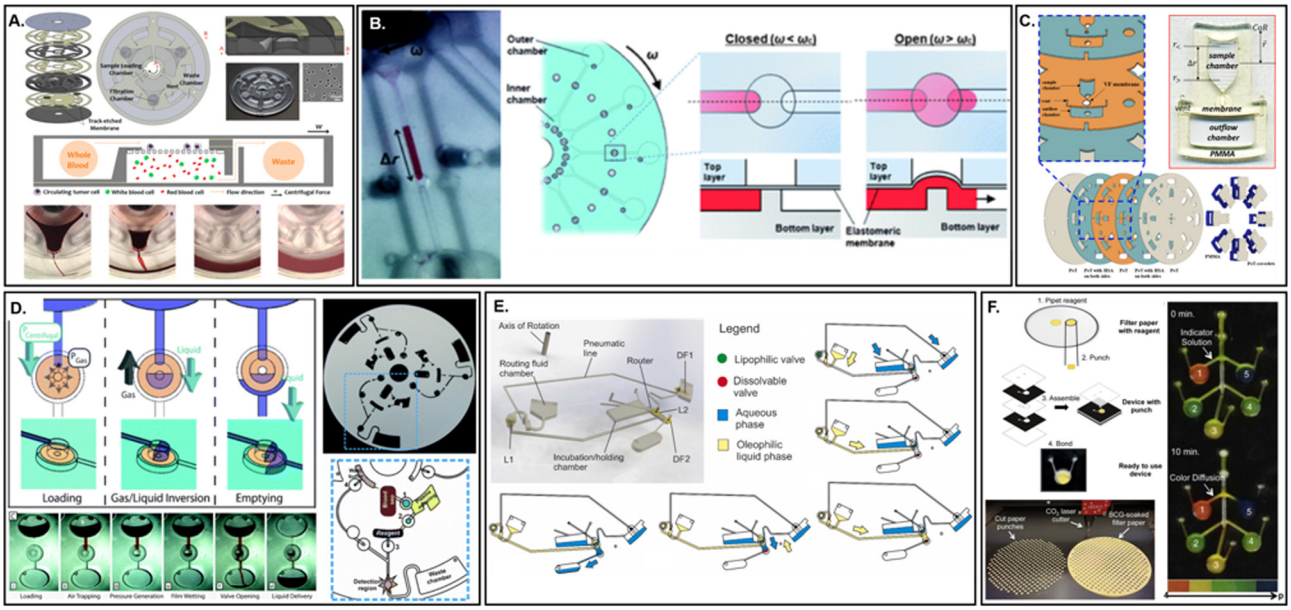

Fig. 7 Membranes composed of synthetic and naturally derived polymeric membranes. A. A track-etched polycarbonate centrifugal microfluidic device for circulating tumour cell isolation (adapted from ref. 131). B. Elastomeric PDMS membranes for integrated valving (adapted from ref. 146). C. Orthogonal flow centrifugal microdevice with cellulose nitrate membrane for detection of Ebola virus-like particles (adapted from ref. 37). D. Water-soluble membranes for programmable valving on a centrifugal platform (adapted from ref. 184). E. Lipophilic dissolvable Parafilm membrane for event-triggered valving during rapid antigenic protein *in situ* display (RAPID) ELISA (adapted from ref. 185). F. Hybrid polyester-cellulose centrifugal microfluidic device for colorimetric indicator reagent storage (adapted from ref. 188).

Among the commercially available synthetic polymer membranes, planar PLMs enable higher sample throughput, while simultaneously minimizing channeling, in comparison to their packed bed counterparts.[134] PLMs may be based on aliphatic polyamides, poly(vinylidene fluoride), or poly(ethylene terephthalate) fibers loaded covalently (*e.g.*, *via* amino, carboxylic, or other functional group) or noncovalently with metal (*e.g.*, gold, silver, palladium, *etc.*) or semiconductor (SiO_2, Al_2O_3, *etc.*) nanoparticles.[135] Despite the variety of PLMs already available, their surface chemistries are primarily directed toward standard applications in solid phase extraction. However, the incorporation of novel nanomaterials into membranes is becoming increasingly valuable, due to their exceedingly tuneable properties and improved mass transfer kinetics. Thankfully, customization of PLMs can be facilely achieved through dip coating, drop casting, or electrospinning.[135] One possible downside to these hybrid structures is their randomized fiber network. For applications requiring more predictable physical surface properties, track-etched (TE) membranes offer uniform pore size distributions, tuneable pore geometries, smooth surfaces, and low auto-fluorescence, rendering them highly suitable for high-performance filtration and microscopy imaging.[136] Similar to their metal and silicon membrane counterparts, noble metal nanoparticles can also render TE surfaces suitable for surface enhanced vibrational spectroscopy.[137] Gold-coated TEs are even commercially available, although an associated increase in cost should be noted with the inclusion of noble metals in either thin film or nanoparticle form.

Typically acquired as its organosilicon¶ monomer and separate cross-linking agent, PDMS remains among the most influential commercially available synthetic polymers on the market. First described by Whitesides' group in 1998, PDMS cross-linking offered a revolutionary new process for microdevice fabrication and cost efficient design iteration.[41] Since its inception, PDMS as a membrane material is most often applied for its high gas permeability, permitting the rapid exchange of both the O_2 and CO_2 necessary for sustaining biological studies.[61,68] This is further supported by its inherent biocompatibility and optical transparency. Hydrophobic PDMS surfaces[138] are readily altered to either fine-tune surface wettability, augment chemical resistance, or prevent adhesion of biological molecules *via* plasma oxidation,[139] laser irradiation,[140] or chemical coating.[141,142] Yet even without surface amendment, PDMS is intrinsically capable of selective nanofiltration of organic solvents.[143] However, this mechanism results in significant material swelling, which may affect proper device functioning.[144] Nonetheless, it is this characteristic, as well as its high elasticity, which renders the material particularly useful either as a mechanism for mechanical actuation[145] or for integrated valving (Fig. 7B).[146,147] Beyond swelling, which alters the rate of permeation, several other potential

¶ Organosilicon compounds, such as poly(dimethylsiloxane), are commonly referred to as 'silicones'. Despite the similar spelling, silicone and silicon are entirely distinct materials. Silicon denotes the chemical element, while silicone is a synthetic substance made using silicon. Silicon binds readily to oxygen, forming silicon dioxide – better known as silica or quartz.

 This journal is © The Royal Society of Chemistry 2023

Open Access Article. Published on 26 June 2023. Downloaded on 10/28/2025 9:16:10 PM. This article is licensed under a Creative Commons Attribution 3.0 Unported Licence.

downsides exist for the use of PDMS as a membrane. Surface modifications are not necessarily permanent and can drive up the cost and complexity of fabrication. Furthermore, residual un-crosslinked oligomers can leach from the surface, acting as a source of contamination.[148] Finally, PDMS degrades with age, eventually affecting its optical and mechanical properties, nor is not particularly resistant to elevated temperatures.

Although PDMS does offer a level of inherent chemical separation due to its tuneable porosity and wetting characteristics,[149] similar to many other membrane materials, highly selective discrimination is not possible without additional surface functionalization. However, molecularly imprinted polymers represent a unique category of discerning membranes, possessing molecular-level recognition sites reminiscent of some biological compounds (*e.g.*, aptamers, antibodies, or affibodies). Highly versatile, MOIs can be generated against a diverse array of targets with different structures, sizes, and physicochemical properties. As a membrane material, MIPs are considered relatively inexpensive, physically and chemically stable (although chemical compatibility can be an important limiting factor), and reusable.[150] Preparation of MIPs can be achieved *via* several methods, including suspension, emulsion, and sol–gel formation.[151,152] Importantly, many of these procedures are single-step reactions with high yields and will also determine whether the resulting structure is self-supported or must act as a supported membrane.[152,153] Although the variety of available preparative techniques yields exceptional customization capabilities in flux capacity and surface functionality, the synthesis parameters are most commonly obtained experimentally. The result is a time-consuming and laborious optimization path, which has so far been the major roadblock to greater MIP advocacy and application.[154,155] Even so, given the explosion in microfluidic sensors, coupled with the intensity of research within the field aimed at improving preparation methods through computational simulations,[154] MIPs are expected to fulfil an urgent need in the development of low-cost, highly stable, and highly selective microdevices.[150] Centrifugal microdevices could possibly offer a solution for automating high throughput screening of optimum sol–gel synthesis parameters *via* repeated architecture.[150] A key aspect for researchers to avoid will be a recurrence of the difficulty in industrial scale-up methods for microdevices which incorporate MIPs. The difficulty of mass manufacture remains a roadblock for PDMS-based microdevices to this day, and should serve as a cautionary tale during conception of MIP-based microdevice fabrication.

In contrast to MIPs, fabric membranes represent a promising material for incorporation within microdevices. Fabric membranes may be composed of a variety of hybrid materials depending upon the desired application, including polyester, cellulose, or silica based substrate fibers coated in either commercially available or custom sol–gel inorganic/organic polymers (*e.g.*, PDMS, poly(ethylene glycol), or poly(tetrahydrofuran). Detailed resources within the literature are available for various sol–gel preparation procedures.[156] Thus far, fabric membranes have been most extensively employed for sorptive extraction,[157,158] coined fabric phase sorptive extraction (FPSE), combining two well-known techniques within the field: solid phase extraction and solid phase microextraction.[159] Notably, these materials are capable of extracting analytes without sample modification, minimizing pre-treatment steps and subsequent analyte loss.[160] Sol–gel coated FPSE membranes are chemically and thermally stable due to the covalent bond between the fabric substrate and thin sol–gel coating. This includes exposure to a pH range between 1–13 as well as compatibility to an extensive variety of organic solvents, without affecting the chemical functionality or structural integrity of the hybrid substrate.[161] This stability renders these membranes suitable for a range of downstream analytical processes, including mass spectrometry (MS), gas chromatography (GC), high performance liquid chromatography (HPLC), or capillary electrophoresis (CE).[45,162] Importantly, although fabric sol–gel membranes are not yet commercially available, their precursor substrates are. Furthermore, membrane fabrication strategies (*i.e.*, dip-coating) are eminently accessible and affordable. Although pore size distribution and geometry are not well controlled, two highly desirable characteristics is superior batch-to-batch reproducibility and considerable permeability.[163] This latter property increases the pressure drop (ΔP) experienced by incoming fluid, augmenting their compatibility with the typical angular frequencies (1–50 Hz) employed in centrifugal microdevices. Finally, their minimal solvent requirements, along with fiber or planar structural forms, enhances their potential for automation and portability. Fabric phase membranes offer serious potential for addressing many of the obstacles surrounding macro-to-micro interfaces for sample integration and processing.

Organic polymers

Cellulose is among the most abundant and renewable organic biopolymer available. As a raw material for membrane formation, it is highly prized for its biodegradable characteristics and touted as a sustainable alternative to petroleum-based synthetic polymers. Given the ubiquity of the raw material, as well as the maturity of the paper-processing industry, membranes composed of cellulose are among the most economical options for membrane fabrication and integration. Naturally occurring in the form of fibrils, cellulose may also be prepared as a aerogel, hydrogel, microfiber, or film.[164] Cellulose consists of a single repeating unit, D-glucose, linked by β-1,4-glycosidic bonds.[165] Extensive hydrogen-bonding as well as van der Waals forces between glucans leads to the formation of crystalline microfibrils.[166] This process imparts lightweight, mechanical rigidity while maintaining a flexibility similar to PDMS, although cellulose-based membranes do remain susceptible to compaction.[167] Due to the presence of exposed hydroxyl

Open Access Article. Published on 26 June 2023. Downloaded on 10/28/2025 9:16:10 PM. This article is licensed under a Creative Commons Attribution 3.0 Unported Licence.

groups on the fibril surfaces, cellulose membranes are naturally hydrophilic. Depending upon the intended application, the optical properties for cellulose may be considered non-ideal; inherent surface roughness renders the material opaque while additives during manufacturing can bestow strong autofluorescence.[168] Should only the microdevice itself need to remain transparent, Ma, *et al.* recently demonstrated stable and controllable patterning of cellulose microfibers onto either polymeric or silicate substrates.[169] For applications where the cellulose membrane itself would optimally exhibit some degree of transparency, isorefractive matching has also been demonstrated as a unique means of improving detectability of functionalized gold nanoparticles.[36] Alternatively, cellulose nanofiber (CNF) papers offer superior optical, thermal, and mechanical strength characteristics relative to standard microfiber cellulose.[170] As yet, commercially produced CNF paper remains extremely limited.[171] However, in-house production methods are readily available within the literature, for either chemical or mechanical nanofibrillation of nanofibers, or by way of bacterial biofilm production.[172,173] 3D printing of CNF hydrogels has also been described.[174] As yet, there are no instances in the literature of a centrifugal microfluidic device which makes use of this exciting new material. However, cellulose nanofiber substrates offer an advanced matrix for organ-on-a-disc cell scaffolds,[175] as ultra-thin film sensors, or as a highly selective separations media.[176]

In addition to the diversity in available structural formats, cellulose may be extensively derivatized to impart novel physicochemical properties. Among the possible derivatives, cellulose acetate (CA), cellulose nitrate (CN), mixed cellulose esters (MCE), and regenerated cellulose (RC) are among the most popular. Conveniently, the commercial availability of both cellulose and its ester derivatives is extensive. CA is obtained by reaction of acetic acid with cellulose fibers, leading to acetylation. The resulting material is more heat resistant, less hygroscopic, and has the lowest affinity toward proteins of all the derivatives previously mentioned.[177] However, the process of acetylation renders CA more brittle and, depending upon the degree of substitution, renders the material less biodegradable than pure cellulose.[178] Unlike cellulose, CA is also more soluble in organic solvents. Cellulose nitrate (often misnamed colloquially as nitrocellulose) is actually a thermoplastic most commonly obtained through treatment of cellulose with a mixture of HNO_3 and H_2SO_4.[179] Although highly flammable, as a membrane material it offers high flow rates, low autofluorescence, and very low affinity toward proteins (in contrast to both cellulose and cellulose acetate) (Fig. 7C).[37,180] However, pure NC membranes are rarely available commercially due to its long-term instability. Instead, composites of CA and NC are prepared as CA is far more stable and less flammable. These membranes are more correctly defined as short-chain mixed cellulose esters (MCE). Although these composite membranes exhibit greater binding affinity toward proteins, they are less susceptible to biodegradation[50] and offer a more uniform pore structure. Mixed chain length MCEs are becoming a focus of research as a potential alternative. Substitution with additional long chain acyl moieties can improve MCE mechanical durability, relative to solely short chain moieties, reducing the need for added plasticizers during manufacturing that can become a source of contamination.[181] Finally, RC refers to any cellulose-derived material within which the cellulose was dissolved then, subsequently reformed. RC thin-films, aerogels, and hydrogels are all prepared in this manner. Higher mechanical strength and thermal resistance along with optical transparency and anti-fouling characteristics, can all be achieved by appropriate selection of the dissolution solvent followed by the combination of a coagulant and physical processing strategy.[164,182,183] This dissolution characteristic may even be adeptly leveraged as an automated valving mechanism (Fig. 7D).[184] Unlike their synthetic polymer counterparts (Fig. 7E),[185] thin films that are partially composed of cellulose fibers can be rendered dissolvable in aqueous solutions, which constitute the vast majority of on-disc assays. RC thin-films may also be acquired from such commercial sources as Whatman[186] or SpectraPor®,[187] which provide dialysis membranes according to a wide range of molecular-scale pore sizes.

In general, cellulose and its derivatives are far less thermally, bio-chemically, or mechanically stable relative to the other membrane materials previously discussed as they are subject to combustion, acid hydrolysis, and biodegradation. Cellulose is also simultaneously hydrophilic and hygroscopic, which leads to significant swelling and subsequent reduction in permeability. Additionally, integration within microfluidic devices is typically limited to compressive or adhesive sealing (Fig. 7F),[188] as direct bonding techniques to metal, glass, or other polymers remains underdeveloped.[189] However, the versatility in surface functionality, biodegradability, hydrophilic character, and cost efficiency imply that cellulose-based membranes will remain, and potentially grow, in preference.

Membrane fabrication & microfluidic integration strategies

A contributing factor in the versatility of integrated membranes relates to their disparate morphologies. For example, the integration methods and intended applications of a hollow fiber membrane will differ greatly from a thin film membrane.[190] These morphologies principally dictate the methodological approaches available for microdevice incorporation, while optimal form, dimension, and even orientation are all dictated by function.[191] Yet beyond the physical configuration, several additional characteristics must also be taken into account during device design, including structural and bio-chemical surface stability. Structural stability depends fundamentally upon the fabrication method, with electrospun fibers being especially

 This journal is © The Royal Society of Chemistry 2023

Open Access Article. Published on 26 June 2023. Downloaded on 10/28/2025 9:16:10 PM.
This article is licensed under a Creative Commons Attribution 3.0 Unported Licence.

susceptible to compressive forces.[192–194] Surface stability is a function of both the material as well as any additional surface modifications performed, with enzymatic-functionalized surfaces typically vulnerable to thermal extremes[195] or PDMS hydrophilicity to age.[196] Therefore, each method for membrane insertion within a microfluidic device comes with a unique set of advantages and challenges. No one method vastly outperforms the others. The diversity of techniques merely serves the purpose of enabling the successful assimilation of an extensive array of membrane types into the rapidly expanding suite of microfluidic devices. These various integration approaches can be parsed according to 1) externally prepared and embedded during fabrication, 2) internally prepared during device fabrication, and 3) *in situ* preparation post device fabrication.[61]

Externally prepared embedded membranes

Embedded membranes may be purchased from commercial vendors, purchased and further functionalized, or prepared entirely in-house. Embedding carries several advantages, including straightforward fabrication, low cost, good reproducibility, and flexibility toward membrane morphology and properties. This implies an adaptive design whereby different applications may be accommodated through simple switching of membrane material(s). An essential aspect for successful membrane incorporation is edge sealing. Sealing the boundary between the membrane and microdevice edges can be achieved for embedded membranes *via* compression (Fig. 8A),[197] solvent bonding, or with adhesives. Although simple, compressive sealing can result in liquid penetration between the microdevice contact layers *via* capillary action, depending upon the surface properties of the liquid and bulk material. The application of heat during compression may also result in unwanted warping, further disrupting any seal. Alternative thermal assembly processes, which make use of multiple materials selected for their differential glass transition (T_g) temperatures, may provide a solution in some instances.[198] By comparison, solvent bonding of materials can provide a more robust seal when compared to solely

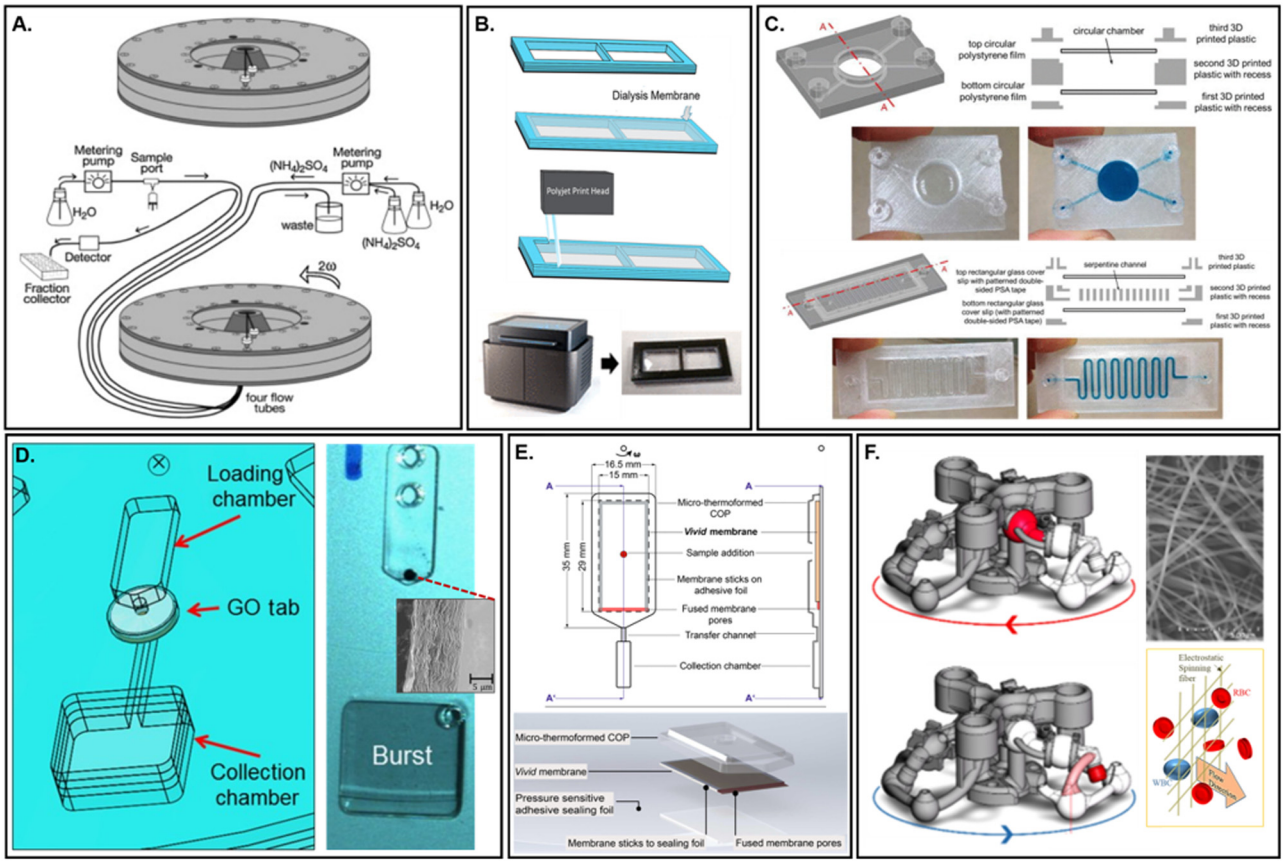

Fig. 8 Externally prepared membranes. A. Compressive sealing of a dialysis membrane used for protein precipitation and chromatography (adapted from ref. 197). B. Print–pause–print method for membrane integration within a microfluidic dialysis device for binding affinity measurements (adapted from ref. 205). C. Print–pause–print embedded cellular acetate membrane within an FDM-based 3D printed microdevice. Membranes were held in place during the remaining print *via* a biocompatible silicone liquid adhesive (adapted from ref. 206). D. Graphene oxide membrane implanted using a pressure sensitive adhesive tab for phase-selective flow control within a centrifugal device (adapted from ref. 114). E. Red blood cell removal through highly asymmetric, commercially available membrane (Vivid™ Plasma Separation) *via* centrifugal actuation. Liquid bypass along membrane edges is prevent with thermal compression during microdevice fabrication (adapted from ref. 207). F. Manually inserted electrospun silicon dioxide membrane within a three-dimensional centrifugal microdevice for blood separation (adapted from ref. 194).

Open Access Article. Published on 26 June 2023. Downloaded on 10/28/2025 9:16:10 PM. This article is licensed under a Creative Commons Attribution 3.0 Unported Licence.

compressive techniques. However, at least one material must be dissolvable by a solvent, typically limiting its usance to synthetic polymers. Application of these solvents also requires an external setup for vapor deposition, or else rely on direct manual application. Solvent entrapment can also lead to local delamination[199] or eventual crazing.[200] Although adhesive sealing offers a broadly applicable and seemingly straightforward approach, membranes may suffer blockages due to liquid adhesive penetration within the pores (*via* lateral wicking) or simply be incompatible with assay reagents. This is especially true for supported liquid membranes (SLM), which may rely on organic solvents for sample extraction. In these instances, inert adhesive tapes, such as silicon, may be feasible.[201]

Several innovative embedding techniques have been successfully demonstrated that attempt to circumvent these particular difficulties. Surface activation, to introduce reactive moieties for covalent linking, offers a high strength sealing method that avoids the potential surface distortion or blockages derived from compressive or liquid adhesive penetration, respectively.[202] Although pore morphology and mass transport are less likely to be affected, surface characteristics may be irreversibly altered. Alternatively, 3D printed devices may incorporate a membrane during fabrication *via* direct implantation.[203,204] This approach can include pausing mid-print during Fused Deposition Modelling (FDM) (Fig. 8B)[205] or through initial placement within the precursor solution during stereolithography (SL) (Fig. 8C),[206] followed by chemical rinsing to remove any non-crosslinked monomer. Avoidance of liquid adhesives, relying instead upon thermo- or pressure-responsive semi-solid adhesives, is a commonplace strategy among laminate structures (Fig. 8D and E).[114,207,208] However, depending upon the microdevice design, these adhesives can introduce contaminants or be otherwise incompatible with the intended microdevice functionality.[209] In these instances, researchers turn to various in-house preparation techniques.

Among the custom membrane fabrication methods available, electrospinning warrants special attention. This membrane fabrication method has become an particularly popular choice due to its convenience, affordability, physicochemical versatility, and mass production compatibility.[210–212] Electrospinning may be employed for the synthesis of nonwoven nanofibers from such disparate materials as organic or synthetic polymers, silica, carbon, and metal.[210,213] An abundance of published fabrication protocols are available for the production of unique nanofibers based primarily on modifications to the high-voltage spinneret, collector, and/or polymer precursor solution.[210,214,215] These fibers may be produced in hollow, core–shell, multichannel, or intrinsically porous morphologies depending upon the material, evaporation rate, feed rate, and solvent miscibility among other parameters.[211,216] Precisely designed functional materials can be produced with this technique, including sol–gels,[217–219] MIPS,[220,221] and nanofibers with embedded nanoparticles.[222,223] Direct surface functionalization, through the attachment of recognition biopolymers (*e.g.*, antibodies, enzyme, or aptamers), is also commonplace.[224,225] The downsides to electrospun membranes include their limited control over pore size and geometry,[226,227] unintended shrinkage or deformation post production,[212] and opacity. However, in the latter case, optical transparency has been demonstrated using specialized protocols.[228] Their biocompatibility, electrical conductivity, or chemical, thermal, and mechanical durability are dependent upon the specific synthesis parameters chosen and therefore vary widely. However, across procedures, electrospun membranes exhibit excellent permeability and high surface capacities. These externally prepared membranes offer similar potential to classic MIPs, with less complex and intensive synthesis optimization required. Additionally, integration of these membranes could employ many of the same methods used for other embedded membrane types. Thus far, the use of electrospun membranes within centrifugal microfluidic devices has been extremely rare (Fig. 8F).[194]

Simultaneously fabricated membranes

Membranes that are prepared within a device during the process of fabrication are able to avoid the complication of sealing disparate materials by virtue of seamless boundaries between the membrane and microdevice channel walls. Often, these membranes are composed of inorganic materials, such as silica, silicon, and alumina. As such, fabrications techniques trace their inspiration directly from the semiconductor industry (*e.g.*, etching or thin film deposition). These techniques offer a high degree of control over feature morphology and pore size, therefore providing high reproducibility in performance. Additionally, feature dimensions down to the tens of nanometers are possible. Finally, as mentioned previously, these materials offer a high degree of thermal stability and chemical resistance. However, as also briefly mentioned, the use of these materials and techniques is limited due to the high cost of materials and relatively sophisticated equipment required. Extensive training for successful fabrication, in addition to cleanroom facilities, may further limit the accessibility of this approach. Recent efforts aimed at addressing some of these drawbacks, namely the elimination of the cleanroom by incorporating additive manufacturing technologies, appear poised to massively broaden the impact of this procedural approach.[229] 3D printing is capable of seamless incorporation of membranes within complex microdevices,[230] through sequential co-printing with different UV-curable resins (Fig. 9A),[231] as well as fabrication of membranes with novel surface patterning (Fig. 9B),[232] thus expanding functionality. Importantly, direct production is achievable in a single step, while the technology itself is highly accessible, making it a competitive option for the next generation of microfluidic membranes. The current downsides included limited resolution and material selection, as well as potential

 This journal is © The Royal Society of Chemistry 2023

Open Access Article. Published on 26 June 2023. Downloaded on 10/28/2025 9:16:10 PM.
This article is licensed under a Creative Commons Attribution 3.0 Unported Licence.

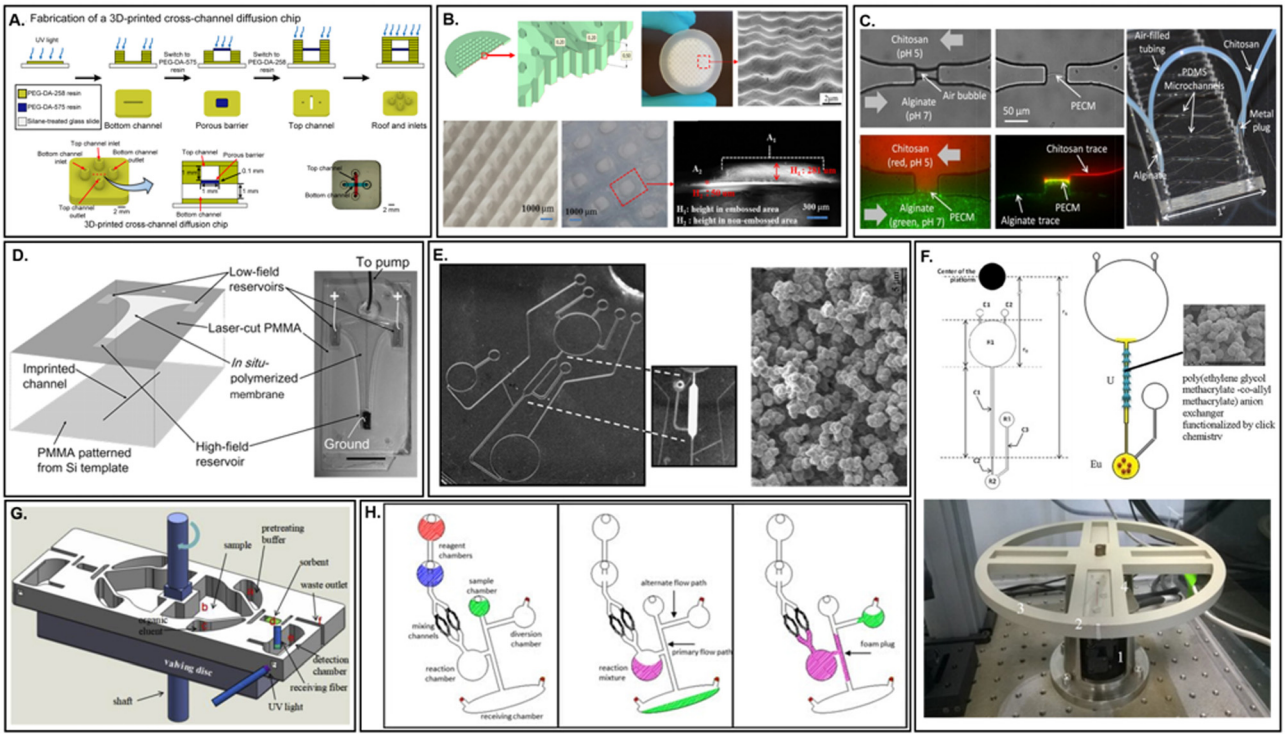

Fig. 9 Simultaneous and *in situ* fabricated membranes. A. Digital manufacturing of porous membranes within 3D printed microdevices through sequential co-printing of multiple resins (adapted from ref. 231). B. 3D printed membranes with surface structures to increase surface area and reduce fouling (adapted from ref. 232). C. Freestanding, *in situ* biopolymer membrane within a PDMS microfluidic device for the creation of small molecule gradients in the absence of protein diffusion (adapted from ref. 191). D. *In situ* polymerized ion-permeable membrane for miniaturized electric field gradient focusing (EFGF) enabling protein preconcentration prior to microchip electrophoresis (adapted from ref. 233). E. *In situ* fabrication of ion-exchange monolithic stationary phases within centrifugal microdevices by microwave-initiated polymerization (adapted from ref. 234). F. Monolithic anion-exchange column within a lab-on-a-CD for chromatographic separation of europium(III) and uranium(VI) (adapted from ref. 236). G. 3D printed porous solid phase extraction sorbent for detection of polycyclic aromatic hydrocarbons in crude oil in a centrifugal duplex cartridge (adapted from ref. 46). H. Formation of a 2D polyurethane foam *via* centrifugal actuation for *in situ* formation of an aqueous-impermeable channel occlusion (adapted from ref. 237).

monomer leaching. According to Clarivate Analytics 'Web of Science', although the number of 3D printed centrifugal microfluidic devices (or centrifugal microdevices which incorporate a 3D printed component) to date remains small, the trajectory for the number of publications *per annum* is rising steadily.

In situ prepared membranes

Membranes prepared *in situ* represent an important compromise between the more costly and complex procedures prevalent with simultaneously fabricated membranes and the minimal costs associated with embedded membranes. Although the available options for commercial membranes are considerable, they are not comprehensive. Novel applications or microdevice configurations may necessitate imaginative membrane properties or orientations, such as those describing interfacial polymerization of vertical membranes (Fig. 9C).[191] Chemical synthesis of these membranes *via* polymerization is a popular response to this need. However, although customizable, reproducibility for membrane integration success or performance across devices may be low as a result of the manual nature of the process. Depending upon the choice in monomer, in addition to the requirements for polymerization initiation, the microdevice may also need to be UV (Fig. 9D)[233] or microwave transparent.[234] Optimization of pore size is usually the result of extensive trial and error.[235] However, *in situ* preparation lacks some of the challenges associated with edge sealing of embedded membranes. Monolithic (Fig. 9E and F),[234,236] 3D printed (Fig. 9G),[46] or foam (Fig. 9H)[237] membranes especially offer an exciting alternative to packed particle columns, which normally require frits or other physical barriers to localize and retain in-channel.

Membrane applications within microfluidic devices

Membrane science and technology is a highly interdisciplinary field. Therefore, it should come as no surprise that the same scientists in pursuit of developing μTAS, with a diverse set of backgrounds, would also embrace such a cross-discipline material to solve

Open Access Article. Published on 26 June 2023. Downloaded on 10/28/2025 9:16:10 PM.
This article is licensed under a Creative Commons Attribution 3.0 Unported Licence.

outstanding challenges within their respective fields.[61,63] Membranes have thus far been used for an impressive array of functions within microfluidic devices, as outlined in Table 1. The following discussion will explore some of the prevailing functions, including reagent storage, mixing, aliquoting, purification, and sensing as applied primarily within centrifugal microfluidic devices. Additional discussion of some emerging uses for membranes, that have notably not received significant attention within the centrifugal microdevice community, will also be included.

Structural applications

Retainment & displacement. Membranes offer an adaptable method for precise control of multiple phases within microfluidic devices. Both restriction and/or allowance of fluidic movement, in the form of valves, has been described many times within the literature. One intuitive method is through mechanical 'pinch valves'[238] which employ elastomeric materials that deflect in response to pressure actuation, applied within or outside the plane of

Table 1 Examples of membranes integrated within centrifugal microfluidic devices. Illustrations provided above the table describe the various fluidic interactions possible *via* centrifugal actuation

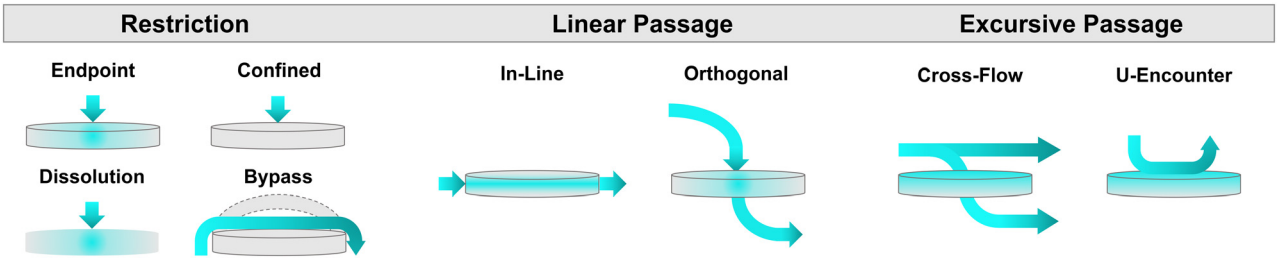

Membrane material	Membrane function	Flow path	Integration strategy	References
Track-etched PC	• Filtration	• Orthogonal	Internal adhesive bonding	75
AAO	• Enrichment	• Orthogonal		
Activated AAO	• Filtration	• Orthogonal	Internal adhesive bonding	76
Glass microfiber	• Reaction chamber • Reagent retainment	• U-encounter • Endpoint	External adhesive attachment	89
Track-etched PC	• Filtration	• Orthogonal	Internal chemical bonding	131
PDMS	• Valving	• Bypass	Internal chemical bonding	146
Cellulose nitrate	• Antigen capture	• Orthogonal	Internal adhesive bonding	37
Cellulose derivatives and plasticizers	• Valving	• Dissolution	Internal adhesive bonding	184
Parafilm	• Valving	• Dissolution	Internal adhesive bonding	185
Cellulose	• Reagent storage	• Endpoint	Adhesive lamination	188
Regenerated cellulose	• Dialysis • Chromatography	• Cross-flow	Compressive sealing	197
Graphene oxide	• Valving	• Orthogonal	Internal adhesive bonding	114
Polysulfone	• Filtration	• In-line	Internal adhesive bonding	207
Electrospun SiO_2	• Filtration	• Orthogonal	Direct insertion	194
Methacrylate monolith	• Extraction	• In-line	*In situ* polymerization	234
Methacrylate monolith	• Extraction	• In-line	*In situ* polymerization	236
Rubber monolith	• Extraction	• In line	Sequential 3D co-printing	46
Polyurethane foam	• Valving	• Confined	*In situ* polymerization	237
Latex	• Valving • Mixing	• Bypass • Confined	Internal adhesive bonding	241
Latex or PDMS	• Valving	• Bypass	Direct insertion	242
PTFE	• Valving	• Confined	Internal adhesive bonding	247
Latex	• Valving	• Confined	Internal adhesive bonding	249
Latex	• Reagent storage • Aliquoting	• Bypass	Compressive sheath	244
PVP-coated Track-etched PC	• Filtration	• Cross-flow	Internal adhesive bonding	252
Track-etched PET	• Cell culture • Perfusion	• Orthogonal • Cross-flow	Solvent bonding	199
Glass microfiber	• Purification	• Orthogonal	Internal adhesive	285
PLM C_{18} silica-PTFE fibrils	• Extraction	• Orthogonal	Internal adhesive	293
Polyester cloth	• Detection	• U-encounter	Thermal sealing	305
Cellulose nitrate	• Detection	• Confined • Orthogonal	Internal adhesive	306
Cellulose	• Filtration • Incubation	• Cross-flow • In-line	Internal adhesive	36
Polyurethane	• Detection	• In-line	Direct insertion	307
Polypropylene	• Supported liquid extraction	• Cross-flow	Internal adhesive	201

 This journal is © The Royal Society of Chemistry 2023

Open Access Article. Published on 26 June 2023. Downloaded on 10/28/2025 9:16:10 PM.
This article is licensed under a Creative Commons Attribution 3.0 Unported Licence.

fluid flow.[239,240] Under these circumstances, membrane deflection may either temporarily or permanently occlude the affected channel(s). Although straightforward, mechanical membrane valves may be creatively adapted to achieve several different fluidic outcomes. In 2018, Aeinehvand *et al.* described a novel method that could be applied toward valving and mixing on the same device (Fig. 10A).[241] In both instances, a latex or nylon elastomeric membrane was deflected *via* external pressure, forcing the membrane into a subterranean channel. Valving was achieved by the inclusion of a sacrificial layer of aluminum foil, which would puncture in response to contact with the deflected membrane, allowing liquid passage. Alternatively, active mixing could be realised by incorporating a metallic microbead above the membrane. By rotating the centrifugal microdevice over a stationary magnet, the bead would automatically deflect the membrane, displacing any fluid below in direct contradiction to the static centrifugal pressure. The impact of this reciprocal fluid mixer was neatly demonstrated by a reduction in total assay time, alongside the enhancement in detection limits, for an integrated ELISA. Active mixing overcomes the reliance on diffusion for analyte mixing within the laminar flow regime. Diffusion is particularly slow for large macromolecules, such as 2° antibodies, with large hydrodynamic radii and correspondingly small coefficients of diffusion. Later, Aeinehvand *et al.* also presented a technique for reversible flow switching within a centrifugal microdevice using elastomeric pinch valves (Fig. 10B).[242] Two separate designs were employed, both requiring a compressible plug made of either rubber or PDMS. In either version, the sealing pressure needed to prevent fluid flow could be calculated based on the rotational frequency of the microdevice and its corresponding applied centrifugal pressure. In one iteration, termed the fixed elastic reversible valve, the plug would resist the pressure of the incoming fluid up to a critical threshold rotational frequency. Once fluid bypassed the valve, increasing angular velocities were required to maintain flow as the length of the liquid column above the valve steadily decreased, a consequence of centrifugal based fluid actuation. Reversibility of the valve is simply achieved by a reduction in rotational frequency, allowing for stepwise fluid transfer. An alternative version, termed the tuneable elastic reversible valve, avoided the need to modulate the angular frequency of the microdevice itself, relying instead upon altering the compression experienced by the elastomeric material through the turning of a screw. By integrating similar valve types onto a single device, automation of complex multi-step bioanalytical assays could be facilitated while still avoiding complex disc fabrication procedures. However, one challenge to the use of programmable valving is the requirement for optimizing the external software and hardware needed to automate their use. In 2016, Aeinehvand *et al.*[243] also demonstrated a manual mechanical valve intended for reagent storage release within a centrifugal microfluidic device. Aqueous liquids retained within bubble wrap were inserted into a source chamber then overlaid with

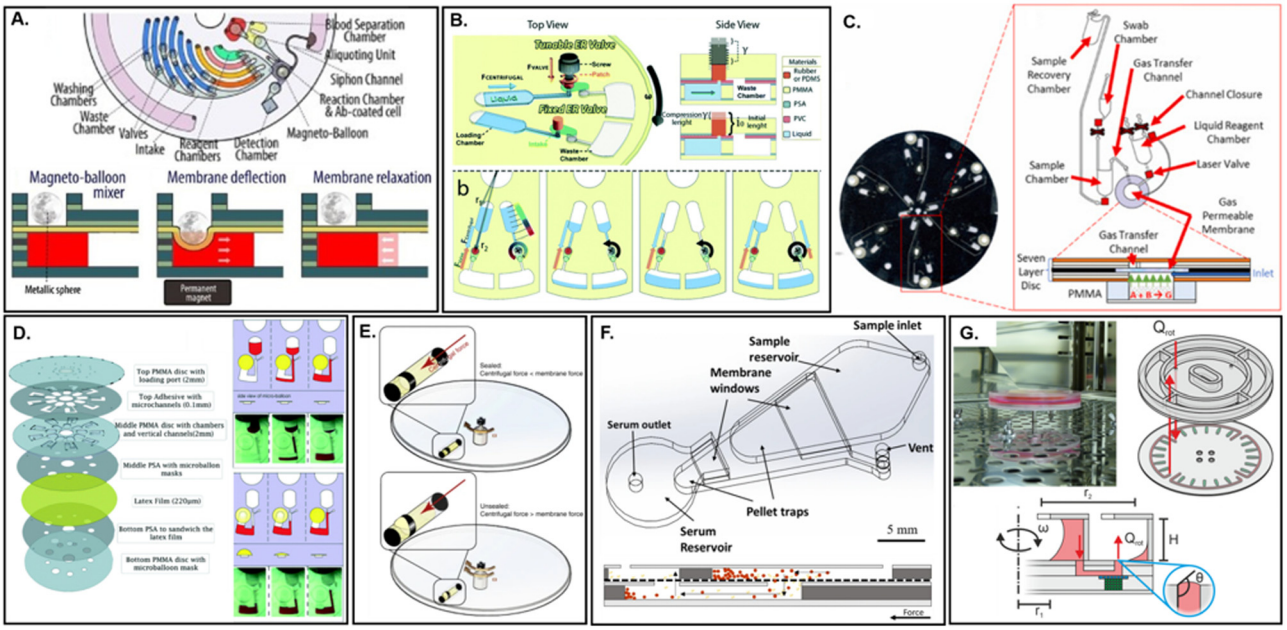

Fig. 10 Structural membrane applications in microfluidic devices. A. Active magneto-balloon mixer and valve based on deflection of a Saran™ wrap membrane for detection of septic shock (adapted from ref. 241). B. Reversible, tunable flow switching within a centrifugal microfluidic device through latex membrane pinch valves (adapted from ref. 242). C. Membrane-modulated centrifugal device for sequestration of reagents used to generate pneumatic pressure for inward fluid displacement (adapted from ref. 247). D. Latex microballoon for liquid pumping on a centrifugal platform (adapted from ref. 249). E. Long term storage and nano- to micro-liter reagent aliquoting through centrifugal actuation of deformable latex membranes (adapted from ref. 244). F. Cross flow filtration of blood samples on a PVP-coated track etched polycarbonate membrane (adapted from ref. 252). G. Track-etched PET membrane for organ-on-a-disc cell culture (adapted from ref. 199).

Open Access Article. Published on 26 June 2023. Downloaded on 10/28/2025 9:16:10 PM. This article is licensed under a Creative Commons Attribution 3.0 Unported Licence.

a latex membrane tab. Manual pressure applied directly to the membrane caused the bubble wrap to burst, releasing the desired reagent within the microchannel architecture. Using this method, centrifugal pressure of ≤106 kPa could be achieved without leaking along with high (92 ± 4%) liquid recovery.

Hydrophobic, air-permeable elastic membranes (*e.g.* latex or PTFE) are also an effective method for retaining either fluids or solids while still allowing gas exchange.[243–245] This can be particularly useful during heating steps which cause fluidic expansion and risk liquid escape.[22,246,247] They may also act as physical barriers capable of avoiding analyst exposure to potentially toxic compounds or contamination of nucleic acid amplification tests (NAATs).[248] Intriguingly, they may also be efficiently leveraged to help generate pneumatic pressure on-disc to drive fluid displacement. Two separate instances where this has been effectively demonstrated on a centrifugal platform include Dignan *et al.* (Fig. 10C)[247] and Aeinehvand *et al.* (Fig. 10D).[249] A common limitation of centrifugal platforms is the inevitable movement of fluid from the center of the microdevice toward its outer edge. This normally enforces a physical limit to the number of processing steps that may be integrated within a single assay according the microdevice radius. However, by integrating a mechanism for fluid displacement back toward the center of rotation, the number of processing steps may be effectively doubled. In the first instance, Dignan *et al.* leveraged an embedded PTFE membrane to retain a tablet of citric acid mixed with sodium bicarbonate. Rehydration of the tablet with deionized water initiated an acid–base neutralization reaction capable of rapidly generating CO_2. This gaseous byproduct was allowed to pass unidirectionally through the membrane and propel ≤10 μL of lysate toward the disc center in ~2 s with 80% recovery, while also precluding any contact between the lysate and the neutralization reaction. Off-disc, this lysate was demonstrated to remain compatible with several downstream NAATs while the reagents necessary for fluid displacement were shown to maintain reactivity even after 6 months of storage on-disc. In contrast, Aeinehvand *et al.* directly employed an elastomeric membrane for potential energy storage in place of chemical reagents. In this case, hydrostatic pressure induced by an incoming fluid within a closed chamber would generate a predictable level of membrane flexion that could be correlated to the changes in fluid levels based on rotational frequency. Ultimately, a relationship between the changing liquid levels, and the reactive pressure exerted by the latex micro-balloon, could be defined. Using this technique, the micro-balloon was found capable of pumping ≤90 μL of deionized water using relatively low (*e.g.*, 1500 rpm) rotational frequencies. The technique was demonstrated for priming of a siphon valve, a commonly employed passive valving mechanism within microfluidic devices. It is significant that the integration of a membrane enabled both Dignan *et al.* and Aeinehvand *et al.* to avoid the need for a 'displacement fluid' which requires either integrated storage near the microdevice center, precisely where available space is at a premium, or immediate pre-addition, which prevents automation. Less commonly, membrane deflection has also been demonstrated for enabling microvolume aliquoting. In 2019, Kazemzadeh *et al.* introduced a liquid-handling technique which offered consistent and precise dispensing of microvolumes on a centrifugal device (Fig. 10E).[244] Latex membranes, which covered the aperture of a sealed FEP ampoule, were bypassed *via* a similar mechanism to Aeinehvand *et al.*, whereby hydrostatic static pressure was generated *via* centrifugal actuation leading to reversible membrane deformation. The critical actuation pressure necessary to achieve liquid dispension were found to depend on three tuneable parameters, which included the membrane thickness and elasticity, as well as the difference between the internal diameter of the membrane alongside the external diameter of the ampoule (*i.e.*, the tightness of seal). However, in contrast to Aeinehvand *et al.*, one additional parameter led to an increase in the required ω beyond a decrease in the liquid plug length. As fluid was dispensed from the ampoule, a partial vacuum was created. This could be accounted for by a liquid dead volume, assuming a known input liquid volume and residual air volume. Finally, simultaneous blood separation and fractioning into separate chambers was demonstrated using a single ampoule outfitted with two membranes while reagent storage stability of even volatile organic compounds (*e.g.*, ethanol) were examined.

Filtration. Filtration can refer either to multi-matter phase separation (*i.e.*, solids from liquids) or physicochemical removal of interfering compounds in a mixture.[250] Mass transport control is normally achieved with the membrane acting as a physical barrier, separating components *via* dimensional exclusion according to a defined pore size, with flow actuated *via* a pressure differential. A major challenge for this application is the flux decline resulting from particle deposition and surface fouling. Although chemical treatments can alter surface properties and thereby effectively mitigate fouling tendency,[251] environmental concerns regarding surface degradation and waste disposal remain. Innovative microstructural alternatives have been proposed which achieve anti-fouling and anti-clogging functionality, in addition to higher durability, through biomimicry.[14] Despite these various challenges, filtration may be a necessary sample processing step in many fields, most particularly biomedical and environmental, where complex mixtures are commonplace. Examples of this include the filtration of soil slurries on a centrifugal microdevice using embedded commercial filters, which outperformed sedimentation for particulate removal.[189] The separation of amphiphilic serum biomarkers from whole blood has also been demonstrated within a centrifugal microfluidic device (Fig. 10F).[252] In this work, Lenz *et al.* were able to purify serum to commercial standards, while simultaneously liberating and preserving amphiphilic biomarkers from host lipoprotein carriers. In many cases, previous efforts aimed at achieving whole blood separation on a microfluidic platform have primarily focused

 This journal is © The Royal Society of Chemistry 2023

Open Access Article. Published on 26 June 2023. Downloaded on 10/28/2025 9:16:10 PM. This article is licensed under a Creative Commons Attribution 3.0 Unported Licence.

on the detection of nucleic acid targets. In contrast, lipidated sugars (*e.g.*, lipopolysaccharide, lipoteichoic acid, *etc.*) are capable of non-specifically adhering to many types of surfaces. Additionally, the integration of fluorescence-based detection methods downstream of filtration may be challenged by accidental lysis of red blood cells (RBCs), causing the release of fluorescent hemoglobin, due to membrane clogging. Lenz *et al.* neatly addressed both challenges by relying on cross-flow filtration over a commercially available, hydrophilic PVP-coated polycarbonate track-etched (PCTE) membrane. By interleaving the PCTE membrane between multiple over- and underlying channels, RBCs were gently removed with extremely high efficiency through a single-step, sequential filtration strategy. Supplementary work describing a pragmatic technique for reproducible integration of the delicate membranes within the microfluidic device were also provided. In brief, water droplets are used to reversibly hold the hydrophilic membrane to the surface of one microdevice layer while a second layer is aligned and secured through a pressure sensitive adhesive. A similar strategy, using methanol to reversibly attach hydrophobic PTFE membranes to microdevice layers during laminate fabrication, has also been used with great success within our own lab.

Finally, an application-agnostic requirement for proper microdevice functioning is the removal of bubbles within microchannels, which can adversely affect fluid dynamics and microdevice performance. The likelihood of bubble formation is particularly high for applications requiring heat, sonication, gaseous reaction byproducts, or with the advent of external fluidic connectors. Several groups have successfully undertaken bubble elimination using either hydrophilic[253] or hydrophobic[254] nanoporous membranes, which take advantage of the separate wetting behaviour of the two-phase system. In these instances, membrane integration was found to be cost efficient and straightforward, with the added design flexibility of operating in two distinct configuration modes (*e.g.*, cross-flow or dead-end). A novel class of photo-switchable 'smart' membranes now offers a non-contact means of altering membrane behavior, including multi-phase permeability, with exciting potential for configurable gating during chemical or biological separations.[255] Thus far, examples of their use within centrifugal microfluidic devices remain scarce to non-existent.

Culturing scaffold. Live cell or tissue studies performed within microfluidic devices often make use of membranes which act as physical supports, while simultaneously enabling the perfusion of nutrients or probes and removal of waste.[13,256–258] Physically isolated but chemically communicating compartments are necessary to investigate cell culturing conditions, perform toxicity tests, or better understand drug permeability in living systems. Both externally embedded, as well as *in situ* fabricated, membranes have been demonstrated, with the most common materials of choice being PDMS, polycarbonate, and photoresist SU-8.[191,212] These integrated membranes also underpin the physiologically accurate recreation and functioning of entire organ or tissue systems. Such microdevices, normally described as tissue/organ/body-on-a-chip, represent the next generation in precision medicine as well as the hopeful replacement for costly and time-consuming animal models in drug discovery studies.[259] As mentioned previously, the choice of membrane material (or integration strategy) may negatively impact its intended application, in addition to its potential commercial scalability. Such a consequence can be illustrated with PDMS, an extremely popular choice as a culturing scaffold, where not only uncured oligomers may leach within the culture media, but small hydrophobic molecules (including cell-signalling steroids), may be absorbed within the microchannel walls.[260] Additionally, microfluidic 3D cell culture and organ-on-a-chip platforms currently face numerous obstacles for commercial viability, largely stemming from their fabrication procedures.[199,261,262] Given the incredible range of available membrane substrates and functionalization methods, even these potential issues may be addressed through thoughtful device design. For example, electrospun fibrous membranes offer scalable platforms for 3D cell culture scaffolds,[263] and may represent a superior alternative to PDMS based substrates. One unique demonstration of a centrifugal organ-on-a-disc (OrganDisc) by Schneider *et al.* made use of a commercially available track-etched PET membrane, integrated within a thermoplastic microdevice (Fig. 10G).[199] This design was not only intended to address the transition to mass manufacturing practices, it also demonstrated higher throughput, semi-automated cell culture in practice. Through precise control of the applied angular velocity of the OrganDisc, patient-derived fibroblasts and adipose stem cells could be loaded and compacted into uniform 3D cell constructs. Continuous media perfusion was achieved through slow disc rotation, facilitating diffusion across the PET membrane and mimicking tissue vasculature. A theoretical assessment of the perfusion requirements was performed to ensure conditions of hypergravity were not induced while still balancing the necessary volumetric flow rates (Q). Alterations in chamber geometry, as well as loading of multiple cells types, enabled versatile tissue engineering for multi-cell type structures. There authors were careful to note several key limitations of their particular microdevice design. This included the need to occasionally manually refresh the liquid media and remove effluent. Although larger reservoirs were posited as a potential solution for extending the timeline of continuous media perfusion, an alternative solution could be the centrifugal microdevice platform developed by Ito *et al.* which allowed for the connection of flow-through tubing directly to a spinning platform.[197]

Reagent storage. Due to their high surface area to volume ratio, membranes offer an incredible loading capacity. This property, combined with their material versatility, renders them particularly useful as agents for reagent sequestration

Open Access Article. Published on 26 June 2023. Downloaded on 10/28/2025 9:16:10 PM. This article is licensed under a Creative Commons Attribution 3.0 Unported Licence.

and implies that many reaction precursors can be stored for use as desired within microfluidic devices. This functionality is of critical importance in the development of portative technologies, as stable chemical or biochemical reagent integration is a necessary feature for commercial implementation. Membranes offer a reagent integration strategy that can be particularly amendable to standard manufacturing procedures. Three main approaches exist for this purpose: direct incorporation of the desired reagent by way of membrane submersion, infusion, or deposition,[89,188,264] valved retainment,[244] or functionalization for *in situ* production with the supply of substrate.[265] In the first scenario, reagents can either be desiccated or lyophilized and pre-concentrated for later resuspension, physically isolated as a liquid for later recovery, or allowed to perfuse passively for slow, continuous release over time. In the second scenario, provision of the required reaction substrate, post membrane integration, may be used to provide a secondary substrate for a downstream reaction. This can be an innovative solution for reactions requiring short lived species, such H_2O_2, in a highly localized manner. The substrate production is also readily quenched through simple flow cessation. This last example represents another key area that is overdue for an innovation with membrane-based centrifugal microdevices. Microfluidic immobilized enzyme reactors (μIMERs) have demonstrated impressive capabilities within the field of biocatalysis.[266,267] Immobilizing enzymes on a solid substrate achieves several important benefits, including higher storage stability, improved selectivity, faster reaction kinetics, and reduced autolysis, among other advantages.

Potential energy storage & harvesting. Beyond the storage of bio-chemical reagents, membranes also represent an important substrate for potential energy storage or even power generation on-disc. Although several examples of micropower generators combined with centrifugal microelectromechanical systems (MEMS) have been demonstrated within the literature,[268–271] none have yet made use of integrated membranes as a means of avoiding additional electronic components (*e.g.*, slip rings, electronic circuit boards, induction coils, or permanent magnets). Nevertheless, several examples of membranes integrated within microfluidic chips have been showcased as an effective, low-cost strategy to provide on-board power, with or without added electricity. In one example, a SiO_2/Si membrane was coupled to a piezoelectric film which converted mechanical flexion of the membrane, in response to thermal expansion of an underlying fluid, to electrical energy.[272] One caveat to this design was the requirement for external heating. In contrast to this, an emerging class of membranes, which preclude the requirement for supplementary external power supply beyond fluid actuation, offers potential energy storage in the form of redox potentials. These micro-batteries make use of bipolar membranes which hold a charge differential across the separate faces, thereby maintaining a pH gradient between the anode and cathode.[273–275] These membranes offer an interesting new mechanism for increasing the power density for energy storage within microbatteries. Similarly, charge separation between aqueous solutions of concentrated electrolytes (*e.g.*, KOH, NaCl, or KCl) have made use of commercially available membranes, including cellulose filters,[276] silica-coated aluminum Anodiscs,[277,278] or Nafion™ (a sulfonated tetrafluoroethylene fluoro-copolymer).[279] These micropower generators and fuel cells fundamentally rely on the Gibb's free energy change from mixing,[280] rendering them both cost-effective as well as environmentally friendly. However, a major challenge for this method of power generation occurs in circumstances where the source of flux across the membrane is not pressure, instead relying solely upon concentration gradients. When the removal rate of solvent through the membrane is faster than the inclusion rate of new solvent to the membrane surface, a localized concentration of solute ions results, lowering the driving force across the membrane.[61] The similar phenomena of surface fouling is often solved at the macro scale by invoking active mixing at the surface of the membrane. In the case of microdevices however, effective mixing within the laminar flow regime remains challenging, particularly in a localized region. For this, the use of self-cleaning surfaces, or reorientation of the membrane, may offer a solution in a few scenarios.[281–283]

Bio-chemical processing applications

Extraction, separation, purification & concentration. Outside of filtration, perhaps the most ubiquitous use of membranes in bio-chemistry is for sample extraction. Extraction is a broad term encompassing analyte collection, separation or purification (also described as sample clean up), preconcentration, or some combination thereof.[284] Collection may be achieved either through adsorption within a membrane or through physical collection on the membrane's surface. In the first instance, adsorption may be harnessed for purification and pre-concentration of nucleic acids. An example of this by Choi *et al.* employed a commercially available silica microfiber membrane for the capture of genomic DNA derived from lysed pathogenic bacteria (Fig. 11A).[285] Sequential washing and elution of the target DNA was controlled *via* optofluidic laser valving, with the Coriolis effect leveraged in a bidirectional channel to prevent effluent mixing. DNA yield and purity were measured in reference to a silica spin-column, after removal off-disc, using spectrophotometry and found to be comparable. The primary difference between the microdevice and gold-standard method was the reduction in both time and manual labor using the LoaD. Furthermore, the introduction of a silica membrane also avoided the more complex processes of loading and retaining loose silica microparticles in similar centrifugal platforms.[286]

Although sample analyte collection *via* flow-through of a liquid medium is arguably the most common method

 This journal is © The Royal Society of Chemistry 2023

Open Access Article. Published on 26 June 2023. Downloaded on 10/28/2025 9:16:10 PM.
This article is licensed under a Creative Commons Attribution 3.0 Unported Licence.

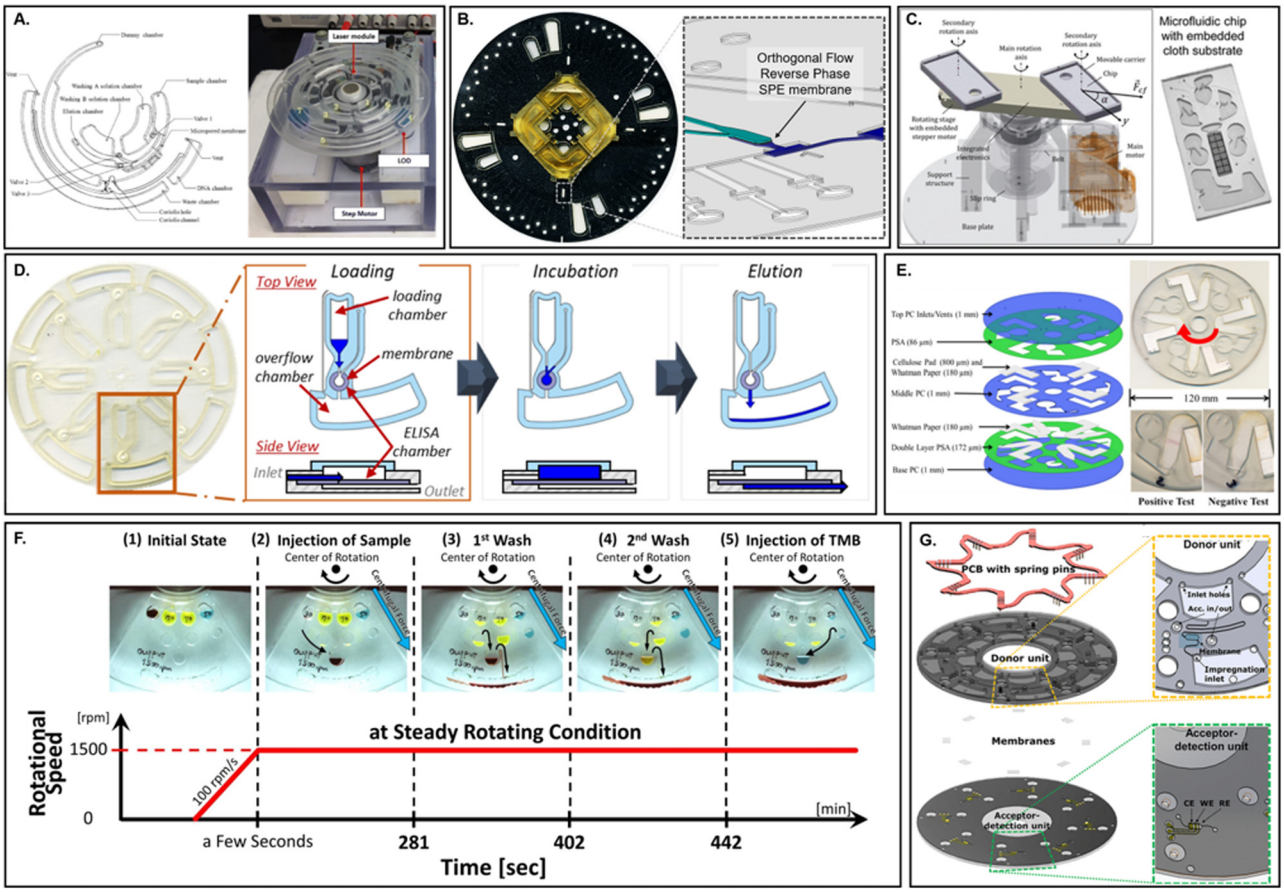

Fig. 11 Bio-chemical membrane applications in microfluidic devices. A. Commercial silica microfiber membrane integrated within a lab on a disk format for automated DNA purification (adapted from ref. 285). B. Enclosed C_{18} surface-functionalized particle loaded membrane for extraction of cannabinoids (adapted from ref. 293). C. Functionalized polyester cloth membranes for colorimetric detection of enterohemorrhagic *Escherichia coli* using an articulated centrifugal platform (adapted from ref. 305). D. Integrated ELISA membrane on a centrifugal microfluidic device for detection of illicit or misused drugs (adapted from ref. 306). E. Supported liquid membrane extraction on a centrifugal microfluidic platform for *in situ* electrochemical detection of bacterial secondary metabolite (adapted from ref. 36). F. Functionalized polyurethane ELISA membrane on an automated LoaD demonstrated with detection of human albumin (adapted from ref. 307). G. Multi-functional surface-modified cellulose membrane insert for simultaneous bacterial pre-concentration and filtration, incubation, and gold nanoparticle based detection with refractive index matching (adapted from ref. 201).

employed within microfluidics, membranes also enable such diverse sample collection procedures as aerosol capture[287] or direct collection from solid surfaces;[288] thus reiterating upon membrane versatility. Notably, in each of the preceding examples, membranes facilitated simpler strategies for world-to-chip interfaces, an essential component in useability. After sample collection, separation of a mixed matrix may be achieved through highly specific capture moieties, such as MIPs or other functionalized surfaces,[165,289] or with more generalized capture techniques including liquid–liquid extraction,[290] supported liquid membrane extraction,[201] solid phase extraction,[291] or dialysis.[197] In these cases, sample collection, separation, and even enrichment may be part of a single-step process rather than a multi-step one. This is particularly powerful for instances where the sample matrix is complex, requiring pre-treatment prior to its introduction in standard analytical chemistry instrumentation. To this end, Andreasen *et al.* miniaturized and partially automated the standard sample pre-treatment technique of supported liquid membrane (SLM) extraction of *p*-coumaric acid produced by *E. coli* (Fig. 11G).[201] The specific detection of the bacterial metabolite by *in situ* electrochemical detection was compared to high-performance liquid chromatography (HPLC) off-disc. In both instances, acidified cell culture supernatant is allowed to interact with an organic phase (dihexyl ether) supported by a commercially available polypropylene membrane.[292] Compounds are separated according to their relative pK_a values as neutral molecules diffuse through the membrane to a neutral aqueous phase on the alternate face. Quantification of *p*-coumaric acid over time by the microdevice system was found to be in good agreement with the HPLC gold standard. Furthermore, the enrichment factor was improved 5-fold when subjected to centrifugal flow actuation as opposed to static conditions.

A separate mechanism for complex sample processing, using solid phase extraction (SPE) *via* a commercially

Open Access Article. Published on 26 June 2023. Downloaded on 10/28/2025 9:16:10 PM. This article is licensed under a Creative Commons Attribution 3.0 Unported Licence.

available particle loaded membrane (PLM),[44] was proposed by O'Connell *et al.* (Fig. 11B).[293] Contrived samples of laced marijuana were subjected to microwave-assisted extraction (MAE), using an acidic solvent contained within a 3D printed cartridge, prior to on-disc attachment. Centrifugal actuation was used to condition the SPE microcolumn prior to the introduction of the solubilized sample. C_{18} functional groups on the membrane surface were found to capture interfering cannabinoids with high efficiency, allowing for downstream detection of illicit lacing agents *via* colorimetry. Importantly, results also indicated that switching from a packed bed SPE format to a PLM raised the microcolumn pressure drop (eqn (3)), and therefore the required angular velocity, enabling simpler integration of downstream assay procedures such as sample metering. Traditionally, porous rigid materials (*e.g.*, potassium silicate or steel) have been employed as physical retainers for solid particles in either column chromatography or enzymatic microreactors; preventing the loss of nano- or microbeads while still allowing eluent passage.[294,295] These frits frequently represented a continuation of the bulk material (*e.g.*, monolithic devices) or had been otherwise conformed or bound to the microchannel walls, creating a tight seal that could withstand significant pressure differentials.[296] However, the inclusion of these frits often represented a significant fabrication challenge for more complex, multi-step microfluidic devices. Therefore, substantial efforts to avoid their obligatory insertion have led to an increasing preference for *in situ* formation of monolithic columns. This can be envisioned as the complete elimination of discrete microparticles, instead expanding the length and lowering the density of what was once functionally a frit into a surface-tuneable "column". In this instance, a commercially available membrane, rather than an *in situ* monolith, was also found to be an effective replacement.

The concentration of analytes within a liquid sample is not limited to solid phase capture and subsequent elution. Evaporative concentration, or simple removal of an interfering solvent, has been performed numerous times by various groups.[297–299] In these examples, the inherent advantages of centrifugal microfluidics for reducing external hardware requirements are emphasized. By applying longer spin cycles, to promote ambient air circulation, the use of an external nitrogen tank for convection-assisted evaporation could be avoided. However, there are many instances where accidental drying of a membrane, through the complete removal of solute *via* centrifugal force, would negative impact membrane functioning for ultrafiltration, preconcentration, or extraction.[300] This hazard is not often discussed within the literature as microdevice design and operation are extensively optimized to avoid its occurrence. Yet, it should be recognized that this particular risk can be eliminated through the incorporation of a physical block, depending upon membrane orientation within the microdevice.[283]

Finally, beyond sample clean up, high resolution analyte separation through chromatography may also be performed on microfluidic devices.[301] By integrating these various sample preparation procedures (*i.e.*, minimizing the number of steps performed and employing limited materials) even complex micro-volume samples may be processed in an automated or near-automated fashion. Additionally, on-line pre-concentration of ultra-low volume samples may also enable detection of trace analytes for downstream mass spectrometry, Surface Enhanced Raman Spectroscopy (SERS), or other gold standard analytical techniques. This is perhaps best exemplified in the field of electrophoresis, where sample preconcentration is accomplished under the influence of an applied voltage. In one example, an ion permeable membrane was interfaced with a separation membrane, for miniaturized electric field gradient focusing (EFGF), demonstrating a capacity to concentrate protein samples up to 10 000-fold in a PMMA microfluidic device.[233] In another example, DNA was preconcentrated *via* retention on a porous silicate membrane for subsequent electrophoretic analysis.[97] For optical detection strategies, where pathlength plays a major role in assay sensitivity, preconcentration within thin (*e.g.*, laminate) microfluidic devices is a necessity for detectability. Analyte localization on a membrane is one such strategy for enhancing detectability. Wiederoder *et al.* presented a hybrid paper–polyester microdevice for a centrifugally controlled colorimetric lateral flow immunoassay (LFA) (Fig. 11E).[36] Relative to a standard LFA, where sample preconcentration is not typically performed, a 100-fold improvement in detecting pathogenic *E. coli* O157:H7 was demonstrated on-disc. An integrated cellulose membrane was initially used to passively remove supernatant derived from centrifugally sedimented bacteria, enriching the target live-cell antigen. Immuno-conjugated gold nanoparticles (AuNPs), combined with the bacterial cell suspension prior to microdevice loading, were further incubated with the sample under constant rotation before deceleration of the microdevice allowed for capillary flow of any AuNP complexes along the functionalized membrane. Silver enhancement and refractive index matching were then performed sequentially on the membrane prior to colorimetric analysis of the LFA test line. In this work, centrifugal force was used to both prevent capillary wicking, thereby extending the incubation period, as well as to reduce the flow rate through the membrane (Q_P), thereby increasing sample residence time.

Detection. Variations of LFAs are among the most common format for membrane-assisted detection, wherein a probe is first immobilized on a detection pad, then later reacted with a target analyte. Unlike standard LFAs, which rely solely on capillary wicking, centrifugal-modulated LFAs may introduce the target analyte using submersive-, dead-end-, or cross-flow behavior to enhance assay performance, prevent membrane clogging, or even facilitate surface regeneration. Although detection strategies are also diverse, they depend principally upon the capture agent and microdevice format, with optical and electrochemical methods predominating. In the first demonstration of a

 This journal is © The Royal Society of Chemistry 2023

Open Access Article. Published on 26 June 2023. Downloaded on 10/28/2025 9:16:10 PM. This article is licensed under a Creative Commons Attribution 3.0 Unported Licence.

membrane used to connect orthogonal channels, Ismagilov *et al.* described a polymeric slip chip featuring an array of crossed channels above and below functionalized membranes.[302] Each channel crossing represented one element of interaction within the array, allowing for combinatorial analysis. The membrane between the channels allowed localization of reaction products between the two continuously flowing reactants, by preventing convective mixing and, therefore, cross-contamination. A downside of the system was the required pressure balancing to control flow across the membrane. More commonly, highly specific capture probes, such as aptamers or antibodies, are used to co-immobilize an agent on the membrane, followed by sandwiching with another specific detection molecule that binds to the target and elicits an optical signal. This signal can be supplied by way of AuNPs[37] or the production of a colored substrate.[208,303,304] Three separate centrifugal microfluidic ELISA devices highlight the suitability of not only the centrifugal platform for this assay type, but also the improved performance metrics through leveraging of membrane technologies. Geissler *et al.* implemented a hybridized, polyester cloth membrane in a singular demonstration of a multi-axis centrifugal platform for the multiplexed detection of eight marker genes in pathogenic *E. coli* (Fig. 11C).[305] All incubation and wash steps were carried out through a fully automated series of spinning and chip reorientation steps, with siphon valve actuation dependent on the chip angle relative to the direction of the centrifugal force. Nucleic acid hybridization on the polyester substrate was determined to be highly specific, cost-effective, rapid (<20 min), and simple to integrate within the thermoformed plastic microdevice. Later, Dignan *et al.* reported the use of an immuno-functionalized cellulose nitrate membrane which directly regulated flow control in a centrifugal microdevice (Fig. 11D).[306] Incubation and wash steps were truncated *via* active mixing on the membrane using low frequency, oscillating spin steps; avoiding any reliance on slow diffusive mixing. Critically, the centrifugal force generated during mixing was insufficient to overcome the liquid entry pressure through the embedded CN membrane. Upon increasing the angular velocity, enough force could be quickly generated to overcome the surface tension within the membrane pores, allowing fluid passage (eqn (4)). Using this strategy, illicit opiates and their metabolites could be reliably differentiated and detected in the ng μL^{-1} range in approximately 1 h. Finally, Okamoto *et al.* provided a unique demonstration of a fully autonomous centrifugal platform that operated at a single rotational frequency (Fig. 11F)[307] using CLOCK (control of liquid operation on centrifugal hydrokinetics) for the detection of human serum albumin. In this concept, the complex multistep assay was automatically controlled through a fluidic circuit, consisting of a water clock network and siphons, which independently executed all required wash and incubation steps. Furthermore, three separate antibody immobilization formats were compared, including direct immobilization to the reaction chamber walls, injection of polystyrene beads, and a polyurethane (PU) foam membrane. The PU membrane was ultimately selected for its superior reaction efficiency, as quantified by the optical density of converted TMB substrate, and convenient handling, as all immobilization procedures could be performed off-disc. Similar to Wiederoder *et al.*,[36] the benefit of precise flow control within embedded membranes (eqn (2)) using a centrifugal platform may be discerned.[35] Flow rates play a major role in optimal detection sensitivity, allowing a balance between sufficient probe–analyte interaction, while disallowing a high degree of nonspecific binding. Control over flow rates can be challenging in passive capillary-based systems, while pneumatic systems may experience pulsing due to syringe pump mechanisms. In contrast, a relationship between the applied spin frequency and resulting flow rate can be calibrated and used for subsequent assay optimization.[37]

Less sensitive to flow rate than ELISA assays, colorimetric chemosensors have made use of both end-point[188,308,309] as well as encounter flow.[89] Johnson *et al.* employed novel optode membranes containing chromoionophores to detect potassium ions in a centrifugal microfluidic device which further implemented calibration steps to eliminate measurement variability between devices. End-point detection in particular avoids the need for flow rate optimization by allowing ample time for reactants to interact. Although this method is less ideal if nonspecific binding and a reduction in the signal to noise ratio may be of concern. The integration of multiple chemosensors within microfluidic devices capable of parallel sample processing can be a particularly powerful tool for the development of sensor arrays which offer greater detection specificity while precluding the need for more expensive affinity-based probes. Other clever methods for membrane assisted optical detection include light-emitting nanofibers as a polarised excitation source,[310] integrated particle counting for the detection of pathogenic bacteria and spores,[311] as well as refractive index matching to detect molecular pollutants in river water.[312] Refractive index matching has been used several times within the literature to enhance the sensitivity of colorimetric based detection on membranes.[36,313] In contrast to planar capture surfaces, porous capture zones allow for reaction site density to be greatly enhanced, with tuning of the membrane pore size altering diffusive interaction characteristics between target and probe compounds. However, light scattering from the membrane structure leads to a severe limitation in assay sensitivity. Index matching fluids have been found to consistently enhance optical performance, both for colorimetric as well as fluorescent assays.[314] Conversely, electrochemical detection methods offer an alternative for highly sensitive detection of multiple analytes simultaneously. The use of a photopatterned biosensor membrane by Moser, *et al.* allowed for the continuous monitoring of glucose, lactate, glutamate, and glutamine without cross-talk, using a microfluidic device

Open Access Article. Published on 26 June 2023. Downloaded on 10/28/2025 9:16:10 PM.
This article is licensed under a Creative Commons Attribution 3.0 Unported Licence.

that could be tailored to separate applications through switching of the photopatterned enzymes.[315]

Finally, each of the preceding detection strategies relied upon functionalized membrane surfaces to provide either an electrochemical or optical readout. However, one underutilized technology for sensitive signal transduction includes the use of microcantilevers.[316] Microcantilevers have been attracting growing interest due to their low-cost batch fabrication methods, simple electronic integration, and versatile detection capabilities. Several examples of membrane-augmented cantilevers have been presented within the literature, whereby deformation of a silicon[317] or polyimide[318] membrane was used to deflect a cantilever either as a generalized pressure sensor or, in the latter case, to monitor pulse waves in healthcare settings. These micromechanical systems are not unlike those of the well-established elastomeric membrane valves[146] and could be used for such applications as in-line monitoring of the flow conditions for cell culture, fluid mixing, droplet manipulation[319] or even direct measurement of live cell layer elasticity.[320]

Conclusions & outlook

From this overview, the versatility and enormous potential of membranes, particularly as integrated functional materials within centrifugal microfluidic devices, should be readily apparent. Additional applications, not discussed in this overview, abound and include everything from membrane-assisted NAAT,[321] micro-fuel cells with membrane-based electrodes[322] or catalysts,[323] as well as protein crystallization and derivitization.[324] However, despite serving as powerful and valuable tools across a wide range of scientific disciplines, membranes also face challenges with regard to their successful integration and use within centrifugal microfluidic devices. This includes difficulties with fabrication procedures related to sealing, their microstructural conformation or surface properties that lead to clogging or fouling, potential susceptibility to compaction, and finally performance declination due to concentration polarization.

As evidenced by the relatively limited number of examples of centrifugal microfluidic devices employing integrated membranes within their construction, ample opportunity remains for exploration using this design framework. The combination of such a versatile material with such an elegant fluidic actuation method may help address the outstanding challenges that remain for addressing some of the most exciting research challenges of this decade as well as for translating these microdevices into the commercial realm, particularly with regard to automating or simplifying sample preparation. Hopefully, this review will serve as a primer for facilitating the expansion of membrane applications within centrifugal microdevices, far beyond their routine employment as filters and valves, to include such areas as cell culture or micropower generators, to mention just a few possibilities.

Author contributions

K. C. O. conceived the original review as well as prepared visualizations and writing. J. P. L. supervised conceptualization and writing. All authors read and approved the completed manuscript.

Conflicts of interest

There are no conflicts to declare.

Acknowledgements

K. C. O. was supported through an internal funding program at the University of Virginia, Charlottesville.

Notes and references

1 N. Convery and N. Gadegaard, *Micro Nano Eng.*, 2019, **2**, 76–91.
2 R. Gorkin, J. Park, J. Siegrist, M. Amasia, B. Seok Lee, J.-M. Park, J. Kim, H. Kim, M. Madou and Y.-K. Cho, *Lab Chip*, 2010, **10**, 1758–1773.
3 J. P. Landers, *Anal. Chem.*, 2003, **75**, 2919–2927.
4 G. M. Whitesides, *Nature*, 2006, **442**, 368–373.
5 S. C. Terry, J. H. Jerman and J. B. Angell, *IEEE Trans. Electron Devices*, 1979, **26**, 1880–1886.
6 C. A. Burtis, J. C. Mailen, W. F. Johnson, C. D. Scott, T. O. Tiffany and N. G. Anderson, *Clin. Chem.*, 1972, **18**, 753–761.
7 C. Regnault, D. S. Dheeman and A. Hochstetter, *High-Throughput*, 2018, **7**, 18.
8 H.-Y. Liu, C. Koch, A. Haller, S. A. Joosse, R. Kumar, M. J. Vellekoop, L. J. Horst, L. Keller, A. Babayan, A. V. Failla, J. Jensen, S. Peine, F. Keplinger, H. Fuchs, K. Pantel and M. Hirtz, *Adv. Biosyst.*, 2020, **4**, 1900162.
9 E. Reátegui, K. E. van der Vos, C. P. Lai, M. Zeinali, N. A. Atai, B. Aldikacti, F. P. Floyd, A. H. Khankhel, V. Thapar, F. H. Hochberg, L. V. Sequist, B. V. Nahed, B. S. Carter, M. Toner, L. Balaj, D. T. Ting, X. O. Breakefield and S. L. Stott, *Nat. Commun.*, 2018, **9**, 175.
10 R. L. Nouwairi, K. C. O'Connell, L. M. Gunnoe and J. P. Landers, *Anal. Chem.*, 2021, **93**, 367–387.
11 S. Sun, L. Jin, Y. Zheng and J. Zhu, *Nat. Commun.*, 2022, **13**, 5481.
12 X. Chen and H. Lv, *NPG Asia Mater.*, 2022, **14**, 1–20.
13 M. A. Catterton, A. F. Dunn and R. R. Pompano, *Lab Chip*, 2018, **18**, 2003–2012.
14 H. Li, A. Raza, S. Yuan, F. AlMarzooqi, N. X. Fang and T. Zhang, *Sci. Rep.*, 2022, **12**, 8178.
15 In *Coulson and Richardson's Chemical Engineering*, ed. R. Chhabra and V. Shankar, Butterworth-Heinemann, 7th edn, 2018, pp. 529–546.
16 J. Azimi-Boulali, M. Madadelahi, M. J. Madou and S. O. Martinez-Chapa, *Micromachines*, 2020, **11**, 603.

 This journal is © The Royal Society of Chemistry 2023

Open Access Article. Published on 26 June 2023. Downloaded on 10/28/2025 9:16:10 PM.
This article is licensed under a Creative Commons Attribution 3.0 Unported Licence.

17 C. Dincer, R. Bruch, E. Costa-Rama, M. T. Fernández-Abedul, A. Merkoçi, A. Manz, G. A. Urban and F. Güder, *Adv. Mater.*, 2019, **31**, 1806739.
18 K. Smith, in *Membrane Processing*, ed. A. Y. Tamime, Blackwell Publishing Ltd., Oxford, UK, 2012, pp. 1–16.
19 *The New York Times*, 2018.
20 Y. Ouyang, J. Li, C. Phaneuf, P. S. Riehl, C. Forest, M. Begley, D. M. Haverstick and J. P. Landers, *Lab Chip*, 2016, **16**, 377–387.
21 M. Grumann, A. Geipel, L. Riegger, R. Zengerle and J. Ducrée, *Lab Chip*, 2005, **5**, 560–565.
22 M. Focke, F. Stumpf, G. Roth, R. Zengerle and F. von Stetten, *Lab Chip*, 2010, **10**, 3210–3212.
23 D. Mark, P. Weber, S. Lutz, M. Focke, R. Zengerle and F. von Stetten, *Microfluid. Nanofluid.*, 2011, **10**, 1279–1288.
24 A. LaCroix-Fralish, E. J. Templeton, E. D. Salin and C. D. Skinner, *Lab Chip*, 2009, **9**, 3151–3154.
25 R. Boom, C. J. Sol, M. M. Salimans, C. L. Jansen, P. M. Wertheim-van Dillen and J. van der Noordaa, *J. Clin. Microbiol.*, 1990, **28**, 495–503.
26 D. Duffy, H. Gillis, J. Lin, N. Sheppard and G. Kellogg, *Anal. Chem.*, 1999, **71**(20), 4669–4678.
27 M. S. Woolf, L. M. Dignan, H. M. Lewis, C. J. Tomley, A. Q. Nauman and J. P. Landers, *Lab Chip*, 2020, **20**, 1426–1440.
28 J. Ducrée, S. Haeberle, S. Lutz, S. Pausch, F. von Stetten and R. Zengerle, *J. Micromech. Microeng.*, 2007, **17**, S103–S115.
29 M. Madadelahi, L. F. Acosta-Soto, S. Hosseini, S. O. Martinez-Chapa and M. J. Madou, *Lab Chip*, 2020, **20**, 1318–1357.
30 S. Soroori, L. Kulinsky and M. Madou, in *Microfluidics and Microscale Transport Processes*, 2013.
31 T. Brenner, T. Glatzel, R. Zengerle and J. Ducrée, *Lab Chip*, 2005, **5**, 146–150.
32 Y. Deng, J. Fan, S. Zhou, T. Zhou, J. Wu, Y. Li, Z. Liu, M. Xuan and Y. Wu, *Biomicrofluidics*, 2014, **8**, 024101.
33 O. Strohmeier, M. Keller, F. Schwemmer, S. Zehnle, D. Mark, F. von Stetten, R. Zengerle and N. Paust, *Chem. Soc. Rev.*, 2015, **44**, 6187–6229.
34 J. F. Hess, S. Zehnle, P. Juelg, T. Hutzenlaub, R. Zengerle and N. Paust, *Lab Chip*, 2019, **19**, 3745–3770.
35 D. M. Kainz, S. M. Früh, T. Hutzenlaub, R. Zengerle and N. Paust, *Lab Chip*, 2019, **19**, 2718–2727.
36 M. S. Wiederoder, S. Smith, P. Madzivhandila, D. Mager, K. Moodley, D. L. DeVoe and K. J. Land, *Biomicrofluidics*, 2017, **11**, 054101.
37 M. S. Woolf, L. M. Dignan, S. M. Karas, H. M. Lewis, K. C. Hadley, A. Q. Nauman, M. A. Gates-Hollingsworth, D. P. AuCoin, H. R. Green, G. M. Geise and J. P. Landers, *Micromachines*, 2022, **13**, 487.
38 H. Bruus, *Theoretical Microfluidics*, Oxford University Press, 2007.
39 D. C. Duffy, J. C. McDonald, O. J. A. Schueller and G. M. Whitesides, *Anal. Chem.*, 1998, **70**, 4974–4984.
40 B. L. Thompson, Y. Ouyang, G. R. M. Duarte, E. Carrilho, S. T. Krauss and J. P. Landers, *Nat. Protoc.*, 2015, **10**, 875–886.
41 J. C. McDonald, D. C. Duffy, J. R. Anderson, D. T. Chiu, H. Wu, O. J. A. Schueller and G. M. Whitesides, *Electrophoresis*, 2000, **21**, 27–40.
42 F. A. L. Dullien, in *Porous Media*, ed. F. A. L. Dullien, Academic Press, San Diego, 2nd edn, 1992, pp. 117–236.
43 Quartz, ambient, air, monitoring, gas, filtration, AQFA, hydrophilic, **https://www.fishersci.ca/shop/products/quartz-fiber-membrane-filter-without-binder/aqfa8x105**, (accessed February 16, 2023).
44 Empore™ SPE Disks matrix active group C_{18}|Sigma-Aldrich, **https://www.sigmaaldrich.com/US/en/product/supelco/66883u**, (accessed October 9, 2022).
45 A. Kabir, R. Mesa, J. Jurmain and K. G. Furton, *Separations*, 2017, **4**, 21.
46 Y. Zhang, J. Xiang, Y. Wang, Z. Qiao and W. Wang, *Sens. Actuators, B*, 2019, **296**, 126603.
47 A. Klechikov, J. Yu, D. Thomas, T. Sharifi and A. V. Talyzin, *Nanoscale*, 2015, **7**, 15374–15384.
48 J. Mohammadnejad, F. Yazdian, M. Omidi, A. D. Rostami, B. Rasekh and A. Fathinia, *Eng. Life Sci.*, 2018, **18**, 298–307.
49 Nylon Membrane Filters, **https://www.thomassci.com//www.thomassci.com/Membrane/_/Nylon-Membrane-Filters1**, (accessed February 16, 2023).
50 Cellulose Acetate (CA) Membranes|FAQ, **https://www.sterlitech.com/faqs/cellulose-acetate**, (accessed October 11, 2022).
51 A. H. Kamel, A. E.-G. E. Amr, N. S. Abdalla, M. El-Naggar, M. A. Al-Omar, H. M. Alkahtani and A. Y. A. Sayed, *Polymers*, 2019, **11**, 1796.
52 W. Krantz, A. Greenberg, E. Kujundzic, A. Yeo and S. Hosseini, *J. Membr. Sci.*, 2013, **438**, 153–166.
53 E. Duffy, R. Padovani, X. He, R. Gorkin, E. Vereshchagina, J. Ducrée, E. Nesterenko, P. N. Nesterenko, D. Brabazon, B. Paull and M. Vázquez, *Anal. Methods*, 2017, **9**, 1998–2006.
54 D. da S. Biron, J. Bortoluz, M. Zeni, C. P. Bergmann and V. dos Santos, *Mater. Res.*, 2016, **19**, 513–519.
55 S. Whitaker, *Transp. Porous Media*, 1986, **1**, 3–25.
56 B. J. Kirby, *Micro- and Nanoscale Fluid Mechanics: Transport in Microfluidic Devices*, Cambridge University Press, 1st edn, 2012.
57 R. G. Iii, C. E. Nwankire, J. Gaughran, X. Zhang, G. G. Donohoe, M. Rook, R. O'Kennedy and J. Ducrée, *Lab Chip*, 2012, **12**, 2894–2902.
58 T.-H. Kim, M. Lim, J. Park, J. M. Oh, H. Kim, H. Jeong, S. J. Lee, H. C. Park, S. Jung, B. C. Kim, K. Lee, M.-H. Kim, D. Y. Park, G. H. Kim and Y.-K. Cho, *Anal. Chem.*, 2017, **89**, 1155–1162.
59 X. Hou, Y. Hu, A. Grinthal, M. Khan and J. Aizenberg, *Nature*, 2015, **519**, 70–73.
60 H. Kim, M. Lim, J. Y. Kim, S.-J. Shin, Y.-K. Cho and C. H. Cho, *Diagnostics*, 2020, **10**, 249.
61 J. de Jong, R. G. H. Lammertink and M. Wessling, *Lab Chip*, 2006, **6**, 1125–1139.
62 X. Chen and J. Shen, *J. Chem. Technol. Biotechnol.*, 2017, **92**, 271–282.
63 Y. Yuan, Z. Cui, H. Jia and J. Wang, *Sep. Purif. Rev.*, 2022, **51**, 545–562.

Open Access Article. Published on 26 June 2023. Downloaded on 10/28/2025 9:16:10 PM.
This article is licensed under a Creative Commons Attribution 3.0 Unported Licence.

64 T. Maruyama, H. Matsushita, J. Uchida, F. Kubota, N. Kamiya and M. Goto, *Anal. Chem.*, 2004, **76**, 4495–4500.
65 S. Nishat, A. T. Jafry, A. W. Martinez and F. R. Awan, *Sens. Actuators, B*, 2021, **336**, 129681.
66 C. Zhang, Y. Su, Y. Liang and W. Lai, *Biosens. Bioelectron.*, 2020, **168**, 112391.
67 S. M. Mitrovski, L. C. C. Elliott and R. G. Nuzzo, *Langmuir*, 2004, **20**, 6974–6976.
68 A. Wang, S. Moghadasi Boroujeni, P. Schneider, L. Christie, K. Mancuso, S. Andreadis and K. Oh, *Micromachines*, 2021, **12**(5), 482.
69 P. Zamprogno, G. Thoma, V. Cencen, D. Ferrari, B. Putz, J. Michler, G. E. Fantner and O. T. Guenat, *ACS Biomater. Sci. Eng.*, 2021, **7**, 2990–2997.
70 Y. Sueyoshi, T. Hashimoto, M. Yoshikawa and K. Watanabe, *Waste Biomass Valorization*, 2011, **2**, 303–307.
71 Y. Kondo and M. Yoshikawa, *Membrane*, 2001, **26**, 228–230.
72 F. Bunge, C. Habben, S. van den Driesehe and M. J. Vellekoop, in *2018 IEEE Micro Electro Mechanical Systems (MEMS)*, 2018, pp. 1237–1240.
73 B. K. Gale, A. R. Jafek, C. J. Lambert, B. L. Goenner, H. Moghimifam, U. C. Nze and S. K. Kamarapu, *Inventions*, 2018, **3**, 60.
74 S. Yeu, J. D. Lunn, H. M. Rangel and D. F. Shantz, *J. Membr. Sci.*, 2009, **327**, 108–117.
75 H.-K. Woo, V. Sunkara, J. Park, T.-H. Kim, J.-R. Han, C.-J. Kim, H.-I. Choi, Y.-K. Kim and Y.-K. Cho, *ACS Nano*, 2017, **11**, 1360–1370.
76 H.-C. Chang, Y.-H. Chen, A.-T. Lo, S.-S. Hung, S.-L. Lin, I.-N. Chang and J.-C. Lin, *Mater. Res. Innovations*, 2014, **18**, S2-685–S2-690.
77 R. Sharma and B. K. Gale, *Procedia Eng.*, 2011, **25**, 713–716.
78 M. Ł. Górzny, N. L. Opara, V. A. Guzenko, V. J. Cadarso, H. Schift, X. D. Li and C. Padeste, *Micro Nano Eng.*, 2019, **3**, 31–36.
79 R. Behrend, C. Dorn, V. Uhlig and H. Krause, *Energy Procedia*, 2017, **120**, 417–423.
80 T. Cui, J. Fang, A. Zheng, F. Jones and A. Reppond, *Sens. Actuators, B*, 2000, **71**, 228–231.
81 E. Formo, M. S. Yavuz, E. P. Lee, L. Lane and Y. Xia, *J. Mater. Chem.*, 2009, **19**, 3878–3882.
82 K. Ge, Q. Wu, Y. Li and Y. Gu, *Spectrochim. Acta, Part A*, 2022, **271**, 120952.
83 G. Chen, Y. Wang, H. Wang, M. Cong, L. Chen, Y. Yang, Y. Geng, H. Li, S. Xu and W. Xu, *RSC Adv.*, 2014, **4**, 54434–54440.
84 M. Domínguez, M. Centeno, M. Martínez, L. Bobadilla, Ó. Laguna and J. Odriozola, *Chem. Eng. Res. Des.*, 2021, **171**, 13–35.
85 G. C. Bandara, C. A. Heist and V. T. Remcho, *Talanta*, 2018, **176**, 589–594.
86 S. Woo, H. R. Park, J. Park, J. Yi and W. Hwang, *Sci. Rep.*, 2020, **10**, 21413.
87 X. Wang, C. Yan, X. Wang, X. Zhao, C. Shi and C. Ma, *Anal. Bioanal. Chem.*, 2020, **412**, 6927–6938.
88 H. Nagasawa, T. Kagawa, T. Noborio, M. Kanezashi, A. Ogata and T. Tsuru, *J. Am. Chem. Soc.*, 2021, **143**, 35–40.
89 K. O'Connell, N. Lawless, B. Stewart and J. Landers, *Lab Chip*, 2022, **22**, 2549–2565.
90 R. G. Juez, V. Boffa, D. H. A. Blank and J. E. ten Elshof, *J. Membr. Sci.*, 2008, **323**, 347–351.
91 G. E. Yue, M. G. Roper, E. D. Jeffery, C. J. Easley, C. Balchunas, J. P. Landers and J. P. Ferrance, *Lab Chip*, 2005, **5**, 619–627.
92 S. Chen, X. Shi, S. Chinnathambi, H. Wu and N. Hanagata, *Sci. Technol. Adv. Mater.*, 2013, **14**, 015005.
93 3D Printing Materials, **https://formlabs.com/materials/ceramics/**, (accessed October 9, 2022).
94 R. M. Twyman, in *Encyclopedia of Analytical Science*, ed. P. Worsfold, A. Townshend and C. Poole, Elsevier, Oxford, 2nd edn, 2005, pp. 146–153.
95 H. Wang, X. Dong and Y. S. Lin, in *Membrane Reactors for Energy Applications and Basic Chemical Production*, ed. A. Basile, L. Di Paola, F. l. Hai and V. Piemonte, Woodhead Publishing, 2015, pp. 145–186.
96 B. P. Regmi and M. Agah, *Anal. Chem.*, 2018, **90**, 13133–13150.
97 J. Khandurina, S. C. Jacobson, L. C. Waters, R. S. Foote and J. M. Ramsey, *Anal. Chem.*, 1999, **71**, 1815–1819.
98 S. J. Reinholt and A. J. Baeumner, *Angew. Chem., Int. Ed.*, 2014, **53**, 13988–14001.
99 R. S. Foote, J. Khandurina, S. C. Jacobson and J. M. Ramsey, *Anal. Chem.*, 2005, **77**, 57–63.
100 S. M. Lai, C. P. Ng, R. Martin-Aranda and K. L. Yeung, *Microporous Mesoporous Mater.*, 2003, **66**, 239–252.
101 Z. Zhang, G. Huang, Y. Li, X. Chen, Y. Yao, S. Ren, M. Li, Y. Wu and C. An, *Chem. Eng. J.*, 2022, **427**, 131987.
102 N. Sazali, *J. Mater. Sci.*, 2020, **55**, 11052–11070.
103 M. R. Kiani, M. Meshksar, M. A. Makarem and E. Rahimpour, *Top. Catal.*, 2021, DOI: **10.1007/s11244-021-01505-1**.
104 Y. Wu, T. Yan, K. Zhang and Z. Pan, *Adv. Mater. Technol.*, 2021, **6**, 2100643.
105 J. Du, W.-C. Li, Z.-X. Ren, L.-P. Guo and A.-H. Lu, *J. Energy Chem.*, 2020, **42**, 56–61.
106 Y. S. Song, *Carbon*, 2012, **50**, 1417–1421.
107 J. Anjali, V. K. Jose and J.-M. Lee, *J. Mater. Chem. A*, 2019, **7**, 15491–15518.
108 C. Li, J. Yang, L. Zhang, S. Li, Y. Yuan, X. Xiao, X. Fan and C. Song, *Environ. Chem. Lett.*, 2021, **19**, 1457–1475.
109 A. Kryeziu, V. Slovak, J. Parmentier, T. Zelenka and S. Rigolet, *Ind. Crops Prod.*, 2022, **183**, 114961.
110 J. Kim, L. J. Cote and J. Huang, *Acc. Chem. Res.*, 2012, **45**, 1356–1364.
111 L. J. Cote, J. Kim, V. C. Tung, J. Luo, F. Kim and J. Huang, *Pure Appl. Chem.*, 2010, **83**, 95–110.
112 K. Raidongia, A. T. L. Tan and J. Huang, in *Carbon Nanotubes and Graphene*, ed. K. Tanaka and S. Iijima, Elsevier, Oxford, 2nd edn, 2014, pp. 341–374.
113 A. V. Talyzin, T. Hausmaninger, S. You and T. Szabó, *Nanoscale*, 2014, **6**, 272–281.
114 J. Gaughran, D. Boyle, J. Murphy, R. Kelly and J. Ducrée, *Microsyst. Nanoeng.*, 2016, **2**, 1–7.
115 W. Lv, Z. Sheng, Y. Zhu, J. Liu, Y. Lei, R. Zhang, X. Chen and X. Hou, *Microsyst. Nanoeng.*, 2020, **6**, 1–11.

 This journal is © The Royal Society of Chemistry 2023

Open Access Article. Published on 26 June 2023. Downloaded on 10/28/2025 9:16:10 PM.
This article is licensed under a Creative Commons Attribution 3.0 Unported Licence.

116 L. J. Cote, R. Cruz-Silva and J. Huang, *J. Am. Chem. Soc.*, 2009, **131**, 11027–11032.
117 J. F. Rocha, L. Hostert, M. L. M. Bejarano, R. M. Cardoso, M. D. Santos, C. M. Maroneze, M. R. Gongora-Rubio and C. de C. C. Silva, *Nanoscale*, 2021, **13**, 6752–6758.
118 W. S. Hummers Jr. and R. E. Offeman, *J. Am. Chem. Soc.*, 1958, **80**, 1339–1339.
119 H.-P. Boehm, A. Clauss and U. Hofmann, *J. Chim. Phys.*, 1961, **58**, 141–147.
120 X. Chen and H. Wang, *Nat. Nanotechnol.*, 2021, **16**, 226–227.
121 M. Sun and J. Li, *Nano Today*, 2018, **20**, 121–137.
122 D. Krishnan, F. Kim, J. Luo, R. Cruz-Silva, L. J. Cote, H. D. Jang and J. Huang, *Nano Today*, 2012, **7**, 137–152.
123 K. Zhihui and D. Min, *ACS Biomater. Sci. Eng.*, 2022, **8**, 2849–2857.
124 A. Flachot, A. Akbarinia, H. H. Schütt, R. W. Fleming, F. A. Wichmann and K. R. Gegenfurtner, *J. Vis.*, 2022, **22**, 17.
125 H. Cheng, Y. Huang, F. Zhao, C. Yang, P. Zhang, L. Jiang, G. Shi and L. Qu, *Energy Environ. Sci.*, 2018, **11**, 2839–2845.
126 Y. Liang, F. Zhao, Z. Cheng, Y. Deng, Y. Xiao, H. Cheng, P. Zhang, Y. Huang, H. Shao and L. Qu, *Energy Environ. Sci.*, 2018, **11**, 1730–1735.
127 S. Tang, Z. Liu and X. Xiang, *Carbon Lett.*, 2022, **32**, 1395–1410.
128 B. Adhikari, A. Biswas and A. Banerjee, *ACS Appl. Mater. Interfaces*, 2012, **4**, 5472–5482.
129 M. Kutz, *Mechanical Engineers' Handbook*, Wiley, 4th edn, 2015, vol. 1, ISBN: 978-1-118-11282-3.
130 B. G. Thiam, A. El Magri, H. R. Vanaei and S. Vaudreuil, *Polymers*, 2022, **14**, 1023.
131 A. Lee, J. Park, M. Lim, V. Sunkara, S. Y. Kim, G. H. Kim, M.-H. Kim and Y.-K. Cho, *Anal. Chem.*, 2014, **86**, 11349–11356.
132 K. B. Neeves and S. L. Diamond, *Lab Chip*, 2008, **8**, 701–709.
133 S. Srigunapalan, C. Lam, A. R. Wheeler and C. A. Simmons, *Biomicrofluidics*, 2011, **5**, 013409.
134 H. Lingeman and S. J. F. Hoekstra-Oussoren, *J. Chromatogr. B: Biomed. Sci. Appl.*, 1997, **689**, 221–237.
135 M. C. Díaz-Liñán, A. I. López-Lorente, R. Lucena and S. Cárdenas, in *Solid-Phase Extraction*, ed. C. F. Poole, Elsevier, 2020, pp. 341–354.
136 P. Apel, *Radiat. Meas.*, 2001, **34**, 559–566.
137 B. Krafft, R. Panneerselvam, D. Geissler and D. Belder, *Anal. Bioanal. Chem.*, 2020, **412**, 267–277.
138 T. Trantidou, Y. Elani, E. Parsons and O. Ces, *Microsyst. Nanoeng.*, 2017, **3**, 1–9.
139 B. Kim, E. T. K. K. Peterson and I. Papautsky, *Conf. Proc. IEEE Eng. Med. Biol. Soc.*, 2004, **2004**, 5013–5016.
140 M. T. Khorasani and H. Mirzadeh, *J. Biomater. Sci., Polym. Ed.*, 2004, **15**, 59–72.
141 S. H. Cho, J. Godin and Y.-H. Lo, *IEEE Photonics Technol. Lett.*, 2009, **21**, 1057–1059.
142 R. M. Diebold and D. R. Clarke, *Langmuir*, 2012, **28**, 15513–15520.
143 N. Stafie, D. F. Stamatialis and M. Wessling, *Sep. Purif. Technol.*, 2005, **45**, 220–231.
144 K. Keshmiri, H. Huang and N. Nazemifard, *SN Appl. Sci.*, 2019, **1**, 711.
145 C. V. Rumens, M. A. Ziai, K. E. Belsey, J. C. Batchelor and S. J. Holder, *J. Mater. Chem. C*, 2015, **3**, 10091–10098.
146 H. Hwang, H.-H. Kim and Y.-K. Cho, *Lab Chip*, 2011, **11**, 1434–1436.
147 J. Goldowsky and H. F. Knapp, *RSC Adv.*, 2013, **3**, 17968–17976.
148 Y. Wang, S. Chen, H. Sun, L. Wanbo, C. Hu and K. Ren, *Microphysiological Systems*, 2018, **2**, 6.
149 M. Abshirini, M. C. Saha, M. Cengiz Altan and Y. Liu, *Mater. Des.*, 2021, **212**, 110194.
150 Y. Saylan and A. Denizli, *Micromachines*, 2019, **10**, 766.
151 Y. L. Mustafa, A. Keirouz and H. S. Leese, *J. Mater. Chem. B*, 2022, **10**, 7418–7449.
152 C.-C. Hong, C.-P. Chen, J.-C. Horng and S.-Y. Chen, *Biosens. Bioelectron.*, 2013, **50**, 425–430.
153 M. Yoshikawa, K. Tharpa and Ș.-O. Dima, *Chem. Rev.*, 2016, **116**, 11500–11528.
154 Z. Liu, Z. Xu, D. Wang, Y. Yang, Y. Duan, L. Ma, T. Lin and H. Liu, *Polymers*, 2021, **13**, 2657.
155 E. Turiel and A. M. Esteban, in *Solid-Phase Extraction*, ed. C. F. Poole, Elsevier, 2020.
156 A. Kabir, K. G. Furton and A. Malik, *TrAC, Trends Anal. Chem.*, 2013, **45**, 197–218.
157 S. Santana-Viera, A. Canino-Byreing, M. E. Torres-Padrón, Z. Sosa-Ferrera, J. J. Santana-Rodríguez, A. Kabir and K. G. Furton, *Separations*, 2022, **9**, 69.
158 N. P. Kalogiouri, A. Kabir, B. Olayanju, K. G. Furton and V. F. Samanidou, *J. Chromatogr. A*, 2022, **1664**, 462785.
159 R. Kumar, Gaurav, Heena, A. K. Malik, A. Kabir and K. G. Furton, *J. Chromatogr. A*, 2014, **1359**, 16–25.
160 A. Kabir and K. G. Furton, in *Solid-Phase Extraction*, ed. C. F. Poole, Elsevier, 2020.
161 A. Kabir and V. Samanidou, *Molecules*, 2021, **26**, 865.
162 A. Taraboletti, M. Goudarzi, A. Kabir, B. Moon, E. Laiakis, J. Lacombe, P. Ake, S. Shoishiro, D. Brenner, A. Fornace and F. Zenhausem, *Journal of Proteome Research*, 2019, **18**(8), 3020–3031.
163 V. Samanidou and A. Kabir, *Analytica*, 2022, **3**, 439–447.
164 Y. Guo, L. Cai, G. Guo, H. Xie, L. Zhang, L. Jin, S. Liang, L. Hu, Q. Xu and Q. Zheng, *ACS Sustainable Chem. Eng.*, 2021, **9**, 11847–11854.
165 Y. Nakai and M. Yoshikawa, *Polym. J.*, 2015, **47**, 334–339.
166 S. Rongpipi, D. Ye, E. D. Gomez and E. W. Gomez, *Front. Plant Sci.*, 2019, **9**, DOI: **10.3389/fpls.2018.01894**.
167 S. Moran, in *An Applied Guide to Water and Effluent Treatment Plant Design*, ed. S. Moran, Butterworth-Heinemann, 2018, pp. 69–100.
168 J. Hiltunen, C. Liedert, M. Hiltunen, O.-H. Huttunen, J. Hiitola-Keinänen, S. Aikio, M. Harjanne, M. Kurkinen, L. Hakalahti and L. P. Lee, *Lab Chip*, 2018, **18**, 1552–1559.

Open Access Article. Published on 26 June 2023. Downloaded on 10/28/2025 9:16:10 PM.
This article is licensed under a Creative Commons Attribution 3.0 Unported Licence.

169 P. Ma, S. Wang, J. Wang, Y. Wang, Y. Dong, S. Li, H. Su, P. Chen, X. Feng, Y. Li, W. Du and B.-F. Liu, *Anal. Chem.*, 2022, **94**, 13332–13341.
170 O. Nechyporchuk, M. N. Belgacem and J. Bras, *Ind. Crops Prod.*, 2016, **93**, 2–25.
171 Cellulose Nanofiber|PRODUCTS|Nippon Paper Group, **https://www.nipponpapergroup.com/english/products/cnf/**, (accessed February 15, 2023).
172 M.-C. Hsieh, H. Koga, K. Suganuma and M. Nogi, *Sci. Rep.*, 2017, **7**, 41590.
173 S. Wang, T. Li, C. Chen, W. Kong, S. Zhu, J. Dai, A. J. Diaz, E. Hitz, S. D. Solares, T. Li and L. Hu, *Adv. Funct. Mater.*, 2018, **28**, 1707491.
174 S. Shin and J. Hyun, *ACS Appl. Mater. Interfaces*, 2017, **9**, 26438–26446.
175 G. F. Picheth, C. L. Pirich, M. R. Sierakowski, M. A. Woehl, C. N. Sakakibara, C. F. de Souza, A. A. Martin, R. da Silva and R. A. de Freitas, *Int. J. Biol. Macromol.*, 2017, **104**, 97–106.
176 C. Chen, C. Zhu, Y. Huang, Y. Nie, J. Yang, R. Shen and D. Sun, *Carbohydr. Polym.*, 2016, **137**, 271–276.
177 M. Bhansali, N. Dabholkar, P. Swetha, S. K. Dubey and G. Singhvi, in *Modeling and Control of Drug Delivery Systems*, ed. A. T. Azar, Academic Press, 2021, pp. 313–331.
178 M. Niaounakis, in *Management of Marine Plastic Debris*, ed. M. Niaounakis, William Andrew Publishing, 2017, pp. 1–55.
179 T. Heinze and T. Liebert, in *Polymer Science: A Comprehensive Reference*, ed. K. Matyjaszewski and M. Möller, Elsevier, Amsterdam, 2012, pp. 83–152.
180 J. G. McNally and W. Vanselow, *J. Am. Chem. Soc.*, 1930, **52**, 3846–3856.
181 S. Tanaka, T. Iwata and M. Iji, *ACS Sustainable Chem. Eng.*, 2017, **5**, 1485–1493.
182 H. Tu, M. Zhu, B. Duan and L. Zhang, *Adv. Mater.*, 2021, **33**, 2000682.
183 X. Huang, F. Tian, G. Chen, F. Wang, R. Weng and B. Xi, *Membranes*, 2021, **12**, 42.
184 R. Gorkin III, C. E. Nwankire, J. Gaughran, X. Zhang, G. G. Donohoe, M. Rook, R. O'Kennedy and J. Ducrée, *Lab Chip*, 2012, **12**, 2894–2902.
185 R. Mishra, R. Alam, D. McAuley, T. Bharaj, D. Chung, D. J. Kinahan, C. Nwankire, K. S. Anderson and J. Ducrée, *Sens. Actuators, B*, 2022, **356**, 131305.
186 Whatman Regenerated Cellulose Membranes - MEMBRANE, RC55 0.45UM 50MM 100/PK - 10410214100 Each/Pack, **https://www.graylinemedical.com/products/whatman-regenerated-cellulose-membranes-membrane-rc55-0-45um-50mm-100pk-10410214**, (accessed May 29, 2023).
187 SpectraPor® (1–4) —DRY – Standard RC single-layer membrane – Defimedica, **https://www.defimedica.com/technologies/spectrapor-1-4-dry-standard-rc-single-layer-membrane**, (accessed May 29, 2023).
188 S. T. Krauss, V. C. Holt and J. P. Landers, *Sens. Actuators, B*, 2017, **246**, 740–747.
189 E. J. Templeton and E. D. Salin, *Microfluid. Nanofluid.*, 2014, **17**, 245–251.
190 N. Torto, J. Bång, S. Richardson, G. S. Nilsson, L. Gorton, T. Laurell and G. Marko-Varga, *J. Chromatogr. A*, 1998, **806**, 265–278.
191 X. Luo, H.-C. Wu, J. Betz, G. W. Rubloff and W. E. Bentley, *Biochem. Eng. J.*, 2014, **89**, 2–9.
192 L. T. Choong, M. M. Mannarino, S. Basu and G. C. Rutledge, *J. Mater. Sci.*, 2013, **48**, 7827–7836.
193 S. M. Giannitelli, M. Costantini, F. Basoli, M. Trombetta and A. Rainer, *Electrofluidodyn. Technol. (EFDTs) Biomater. Med. Devices*, 2018, 139–155.
194 X. Qin, H. Chen, S. Jia and W. Wang, *Microsyst. Technol.*, 2021, **27**, 2639–2646.
195 B. Koh and K. R. Kim, *ACS Omega*, 2019, **4**, 15134–15138.
196 D. Bodas and C. Khan-Malek, *Microelectron. Eng.*, 2006, **83**, 1277–1279.
197 Y. Ito and L. Qi, *J. Chromatogr., B*, 2010, **878**, 154–164.
198 F. I. Uba, B. Hu, K. Weerakoon-Ratnayake, N. Oliver-Calixte and S. A. Soper, *Lab Chip*, 2015, **15**, 1038–1049.
199 S. Schneider, F. Erdemann, O. Schneider, T. Hutschalik and P. Loskill, *APL Bioeng.*, 2020, **4**, 046101.
200 S. P. Ng, F. E. Wiria and N. B. Tay, *Procedia Eng.*, 2016, **141**, 130–137.
201 S. Z. Andreasen, K. Sanger, C. B. Jendresen, A. T. Nielsen, J. Emnéus, A. Boisen and K. Zór, *ACS Sens.*, 2019, **4**, 398–405.
202 K. Aran, L. A. Sasso, N. Kamdar and J. D. Zahn, *Lab Chip*, 2010, **10**, 548–552.
203 F. Li, N. P. Macdonald, R. M. Guijt and M. C. Breadmore, *Lab Chip*, 2019, **19**, 35–49.
204 K. Ikuta, S. Maruo, T. Fujisawa and A. Yamada, in *Technical Digest. IEEE International MEMS 99 Conference. Twelfth IEEE International Conference on Micro Electro Mechanical Systems (Cat. No.99CH36291)*, 1999, pp. 376–381.
205 C. W. Pinger, A. A. Heller and D. M. Spence, *Anal. Chem.*, 2017, **89**, 7302–7306.
206 P. K. Yuen, *Biomicrofluidics*, 2016, **10**, 044104.
207 S. Hin, M. Loskyll, V. Klein, M. Keller, O. Strohmeier, F. von Stetten, R. Zengerle and K. Mitsakakis, *Microelectron. Eng.*, 2018, **187–188**, 78–83.
208 J.-E. Kim, J.-H. Cho and S.-H. Paek, *Anal. Chem.*, 2005, **77**, 7901–7907.
209 H. Mohamed, A. P. Russo, D. H. Szarowski, E. McDonnell, L. A. Lepak, M. G. Spencer, D. L. Martin, M. Caggana and J. N. Turner, *J. Chromatogr. A*, 2006, **1111**, 214–219.
210 H. Bagheri, O. Rezvani, S. Zeinali, S. Asgari, T. Aqda and F. Manshaeir, in *Solid-Phase Extraction*, ed. C. F. Poole, Elsevier, 2020.
211 Z. Rezaei and M. Mahmoudifard, *J. Mater. Chem. B*, 2019, **7**, 4602–4619.
212 H. Moghadas, M. S. Saidi, N. Kashaninejad and N.-T. Nguyen, *Biomicrofluidics*, 2018, **12**, 024117.
213 J.-L. Sanchez, D. Pinto and C. Laberty-Robert, *Electrochim. Acta*, 2021, **373**, 137864.
214 A. Valizadeh and S. Mussa Farkhani, *IET Nanobiotechnol.*, 2014, **8**, 83–92.
215 W.-E. Teo, R. Inai and S. Ramakrishna, *Sci. Technol. Adv. Mater.*, 2011, **12**, 013002.

 This journal is © The Royal Society of Chemistry 2023

Open Access Article. Published on 26 June 2023. Downloaded on 10/28/2025 9:16:10 PM.
This article is licensed under a Creative Commons Attribution 3.0 Unported Licence.

216 B. Ding, M. Wang, X. Wang, J. Yu and G. Sun, *Mater. Today*, 2010, **13**, 16–27.
217 G. George, T. Senthil, Z. Luo and S. Anandhan, in *Electrospun Polymers and Composites*, ed. Y. Dong, A. Baji and S. Ramakrishna, Woodhead Publishing, 2021, pp. 689–764.
218 A. Jauri and S. I. A. Razak, *IOP Conf. Ser.: Mater. Sci. Eng.*, 2018, **440**, 012007.
219 R. A. Caruso, J. H. Schattka and A. Greiner, *Adv. Mater.*, 2001, **13**, 1577–1579.
220 I. S. Chronakis, B. Milosevic, A. Frenot and L. Ye, *Macromolecules*, 2006, **39**, 357–361.
221 K. Yoshimatsu, L. Ye, J. Lindberg and I. S. Chronakis, *Biosens. Bioelectron.*, 2008, **23**, 1208–1215.
222 J. Eom, Y. Kwak and C. Nam, *Chemosphere*, 2022, **303**, 135063.
223 W. Shi, W. Lu and L. Jiang, *J. Colloid Interface Sci.*, 2009, **340**, 291–297.
224 J. Britton, C. L. Raston and G. A. Weiss, *Chem. Commun.*, 2016, **52**, 10159–10162.
225 D. Yang, X. Niu, Y. Liu, Y. Wang, X. Gu, L. Song, R. Zhao, L. Ma, Y. Shao and X. Jiang, *Adv. Mater.*, 2008, **20**, 4770–4775.
226 R. Khajavi and M. Abbasipour, in *Electrospun Nanofibers*, ed. M. Afshari, Woodhead Publishing, 2017, pp. 109–123.
227 W. Su, M. Zhang, W. Wei, H. Wang, W. Zhang, Z. Li, M. Tan and Z. Chen, *PeerJ*, 2022, **10**, e13513.
228 Y. Xiao, H. Luo, R. Tang and J. Hou, *Polymers*, 2021, **13**, 506.
229 C. I. Rogers, K. Qaderi, A. T. Woolley and G. P. Nordin, *Biomicrofluidics*, 2015, **9**, 016501.
230 J.-Y. Lee, W. S. Tan, J. An, C. K. Chua, C. Y. Tang, A. G. Fane and T. H. Chong, *J. Membr. Sci.*, 2016, **499**, 480–490.
231 Y. T. Kim, K. Castro, N. Bhattacharjee and A. Folch, *Micromachines*, 2018, **9**, 125.
232 B. G. Thiam, A. El Magri, H. R. Vanaei and S. Vaudreuil, *Polymers*, 2022, **14**, 1023.
233 R. T. Kelly, Y. Li and A. T. Woolley, *Anal. Chem.*, 2006, **78**, 2565–2570.
234 E. A. Moschou, A. D. Nicholson, G. Jia, J. V. Zoval, M. J. Madou, L. G. Bachas and S. Daunert, *Anal. Bioanal. Chem.*, 2006, **385**, 596–605.
235 J. Moorthy and D. J. Beebe, *Lab Chip*, 2003, **3**, 62–66.
236 M. Losno, I. Ferrante, R. Brennetot, J. Varlet, C. Blanc, B. Grenut, E. Amblard, S. Descroix and C. Mariet, *Micromachines*, 2016, **7**, 45.
237 C. P. Clark, M. S. Woolf, S. L. Karstens, H. M. Lewis, A. Q. Nauman and J. P. Landers, *Micromachines*, 2020, **11**, 627.
238 J. Xiang, Z. Cai, Y. Zhang and W. Wang, *Sens. Actuators, B*, 2018, **259**, 325–331.
239 A. R. Abate and D. A. Weitz, *Appl. Phys. Lett.*, 2008, **92**, 243509.
240 Rotary Membrane Valve & Pump for Microfluidic Devices, **https://www.enplaslifetech.com/rmvp/**, (accessed October 12, 2022).
241 M. M. Aeinehvand, R. F. Martins Fernandes, M. F. Jiménez Moreno, V. J. Lara Díaz, M. Madou and S. O. Martinez-Chapa, *Sens. Actuators, B*, 2018, **276**, 429–436.
242 M. M. Aeinehvand, L. Weber, M. Jiménez, A. Palermo, M. Bauer, F. F. Loeffler, F. Ibrahim, F. Breitling, J. Korvink, M. Madou, D. Mager and S. O. Martínez-Chapa, *Lab Chip*, 2019, **19**, 1090–1100.
243 M. M. Aeinehvand, F. Ibrahim and M. J. Madou, in *International Conference for Innovation in Biomedical Engineering and Life Sciences*, ed. F. Ibrahim, J. Usman, M. S. Mohktar and M. Y. Ahmad, Springer Singapore, Singapore, 2016, vol. 56, pp. 269–271.
244 A. Kazemzadeh, A. Eriksson, M. Madou and A. Russom, *Nat. Commun.*, 2019, **10**, 189.
245 A. R. Homann, L. Niebling, S. Zehnle, M. Beutler, L. Delamotte, M.-C. Rothmund, D. Czurratis, K.-D. Beller, R. Zengerle, H. Hoffmann and N. Paust, *Lab Chip*, 2021, **21**, 1540–1548.
246 Y. Liu, C. B. Rauch, R. L. Stevens, R. Lenigk, J. Yang, D. B. Rhine and P. Grodzinski, *Anal. Chem.*, 2002, **74**, 3063–3070.
247 L. M. Dignan, S. M. Karas, I. K. Mighell, W. R. Treene, J. P. Landers and M. S. Woolf, *Anal. Chim. Acta*, 2022, **1221**, 340063.
248 F. Stumpf, F. Schwemmer, T. Hutzenlaub, D. Baumann, O. Strohmeier, G. Dingemanns, G. Simons, C. Sager, L. Plobner, F. von Stetten, R. Zengerle and D. Mark, *Lab Chip*, 2015, **16**, 199–207.
249 M. M. Aeinehvand, F. Ibrahim, S. W. Harun, W. Al-Faqheri, T. H. G. Thio, A. Kazemzadeh and M. Madou, *Lab Chip*, 2014, **14**, 988–997.
250 I. Seder, H. Moon, S. Jin Kang, S. Shin, W. Jong Rhee and S.-J. Kim, *Lab Chip*, 2022, **22**, 3699–3707.
251 F. Yalcinkaya, E. Boyraz, J. Maryska and K. Kucerova, *Materials*, 2020, **13**, 493.
252 K. D. Lenz, S. Jakhar, J. W. Chen, A. S. Anderson, D. C. Purcell, M. O. Ishak, J. F. Harris, L. E. Akhadov, J. Z. Kubicek-Sutherland, P. Nath and H. Mukundan, *Sci. Rep.*, 2021, **11**, 5287.
253 X. Zhu, *Microsyst. Technol.*, 2009, **15**, 1459–1465.
254 H. G. Derami, R. Vundavilli and J. Darabi, *Microsyst. Technol.*, 2017, **23**, 2685–2698.
255 F. P. Nicoletta, D. Cupelli, P. Formoso, G. De Filpo, V. Colella and A. Gugliuzza, *Membranes*, 2012, **2**, 134–197.
256 O. Schneider, L. Zeifang, S. Fuchs, C. Sailer and P. Loskill, *Tissue Eng., Part A*, 2019, **25**, 786–798.
257 D. Huh, B. D. Matthews, A. Mammoto, M. Montoya-Zavala, H. Y. Hsin and D. E. Ingber, *Science*, 2010, **328**, 1662–1668.
258 N. Ferrell, R. R. Desai, A. J. Fleischman, S. Roy, H. D. Humes and W. H. Fissell, *Biotechnol. Bioeng.*, 2010, **107**, 707–716.
259 Y. Quan, M. Sun, Z. Tan, J. C. T. Eijkel, A. van den Berg, A. van der Meer and Y. Xie, *RSC Adv.*, 2020, **10**, 39521–39530.
260 K. J. Regehr, M. Domenech, J. T. Koepsel, K. C. Carver, S. J. Ellison-Zelski, W. L. Murphy, L. A. Schuler, E. T. Alarid and D. J. Beebe, *Lab Chip*, 2009, **9**, 2132–2139.
261 Q. Wu, J. Liu, X. Wang, L. Feng, J. Wu, X. Zhu, W. Wen and X. Gong, *J. Geophys. Res. Planets*, 2020, **19**, 9.
262 S. Schneider, D. Gruner, A. Richter and P. Loskill, *Lab Chip*, 2021, **21**, 1866–1885.

Open Access Article. Published on 26 June 2023. Downloaded on 10/28/2025 9:16:10 PM.
This article is licensed under a Creative Commons Attribution 3.0 Unported Licence.

263 C. Chen, A. D. Townsend, E. A. Hayter, H. M. Birk, S. A. Sell and R. S. Martin, *Anal. Bioanal. Chem.*, 2018, **410**, 3025–3035.
264 P. Thurgood, S. Baratchi, C. Szydzik, A. Mitchell and K. Khoshmanesh, *Lab Chip*, 2017, **17**, 2517–2527.
265 H. Hisamoto, Y. Shimizu, K. Uchiyama, M. Tokeshi, Y. Kikutani, A. Hibara and T. Kitamori, *Anal. Chem.*, 2003, **75**, 350–354.
266 Y. Zhu, Q. Chen, L. Shao, Y. Jia and X. Zhang, *React. Chem. Eng.*, 2019, **5**, 9–32.
267 B. Wouters, S. A. Currivan, N. Abdulhussain, T. Hankemeier and P. J. Schoenmakers, *TrAC, Trends Anal. Chem.*, 2021, **144**, 116419.
268 S. Smith, D. Mager, A. Perebikovsky, E. Shamloo, D. Kinahan, R. Mishra, S. M. Torres Delgado, H. Kido, S. Saha, J. Ducrée, M. Madou, K. Land and J. G. Korvink, *Micromachines*, 2016, **7**, 22.
269 S. Z. Andreasen, D. Kwasny, L. Amato, A. Line Brøgger, F. G. Bosco, K. B. Andersen, W. E. Svendsen and A. Boisen, *RSC Adv.*, 2015, **5**, 17187–17193.
270 S. M. Torres Delgado, J. G. Korvink and D. Mager, *Biosens. Bioelectron.*, 2018, **117**, 464–473.
271 K. Joseph, F. Ibrahim, J. Cho, T. H. G. Thio, W. Al-Faqheri and M. Madou, *PLoS One*, 2015, **10**, e0136519.
272 S. Whalen, M. Thompson, D. Bahr, C. Richards and R. Richards, *Sens. Actuators, A*, 2003, **104**, 290–298.
273 World Intellectual Property Organization, WO2017071320A1, 2017.
274 Z. Yan, R. J. Wycisk, A. S. Metlay, L. Xiao, Y. Yoon, P. N. Pintauro and T. E. Mallouk, *ACS Cent. Sci.*, 2021, **7**, 1028–1035.
275 RALEX® ion exchange membranes for ED, EDI and E-coating|MEGA, **https://www.mega.cz/membranes/**, (accessed February 15, 2023).
276 X. Zhu, T. Zhang, C. Yu, Y. Yang, D. Ye, R. Chen and Q. Liao, *Int. J. Hydrogen Energy*, 2022, **47**, 15065–15073.
277 S. W. Lee, H. J. Kim and D.-K. Kim, *Energies*, 2016, **9**, 49.
278 Whatman Anodisc inorganic filter membrane supported, diam. 25 mm, pore size 0.02 um- pkg of 50 ea Whatman filter, **https://www.sigmaaldrich.com/**, (accessed May 30, 2023).
279 T.-C. Tsai, C.-W. Liu and R.-J. Yang, *Micromachines*, 2016, **7**, 205.
280 N. Wu, Y. Brahmi and A. Colin, *Lab Chip*, 2023, **23**, 1034–1065.
281 W. Shang, X. Li, W. Liu, S. Yue, M. Li, D. von Eiff, F. Sun and A. K. An, *J. Membr. Sci.*, 2021, **622**, 119021.
282 W. Osman, N. Nawi, S. Samsuri, M. Bilad and S. Yusup, *AIP Conf. Proc.*, 2022, 050008.
283 Amicon Ultra-15 Centrifugal Filter 3 kDa MWCO Millipore, **https://www.sigmaaldrich.com/**, (accessed May 29, 2023).
284 S. Tang, H. Zhang and H. K. Lee, *Anal. Chem.*, 2016, **88**, 228–249.
285 M.-S. Choi and J.-C. Yoo, *Appl. Biochem. Biotechnol.*, 2015, **175**, 3778–3787.
286 L. M. Dignan, M. S. Woolf, C. J. Tomley, A. Q. Nauman and J. P. Landers, *Anal. Chem.*, 2021, **93**, 7300–7309.
287 S. Krauss, *PhD*, University of Virginia, 2018.
288 Y. Sameenoi, P. Panymeesamer, N. Supalakorn, K. Koehler, O. Chailapakul, C. S. Henry and J. Volckens, *Environ. Sci. Technol.*, 2013, **47**, 932–940.
289 P.-C. Wang, J. Gao and C. S. Lee, *J. Chromatogr. A*, 2002, **942**, 115–122.
290 Z.-X. Cai, Q. Fang, H.-W. Chen and Z.-L. Fang, *Anal. Chim. Acta*, 2006, **556**, 151–156.
291 S. Kumar, V. Sahore, C. I. Rogers and A. T. Woolley, *Analyst*, 2016, **141**, 1660–1668.
292 Celgard® Microporous Films, **https://aka-mobility.com/product/celgard/**, (accessed May 30, 2023).
293 K. C. O'Connell, M. B. Almeida, R. L. Nouwairi, E. T. Costen, N. K. Lawless, M. E. Charette, B. M. Stewart, S. L. Nixdorf and J. P. Landers, In Prep.
294 J. Koehler and P. Patel, *US Pat.*, US7153421B2, 2006.
295 K. Ö. Hamaloğlu, E. Sağ and A. Tuncel, *J. Photochem. Photobiol., A*, 2017, **332**, 60–65.
296 C. K. Ong, *Ph.D. Thesis*, Department of Chemistry, The University of Hull, 2012.
297 S. Krauss, Chemistry - Graduate School of Arts and Sciences, *PHD (Doctor of Philosophy)*, University of Virginia, 2018.
298 B. H. Timmer, K. M. van Delft, W. Olthuis, P. Bergveld and A. van den Berg, *Sens. Actuators, B*, 2003, **91**, 342–346.
299 J. C. T. Eijkel, J. G. Bomer and A. van den Berg, *Appl. Phys. Lett.*, 2005, **87**, 114103.
300 HyperSep Column Applications, **https://apps.thermoscientific.com/media/cmd/flipbooks/HyperSep-Column-Application-Notebook/files/assets/basic-html/page-1.html**, (accessed May 30, 2023).
301 P. Myers and K. D. Bartle, *J. Chromatogr. A*, 2004, **1044**, 253–258.
302 R. F. Ismagilov, J. M. K. Ng, P. J. A. Kenis and G. M. Whitesides, *Anal. Chem.*, 2001, **73**, 5207–5213.
303 S. Lutz, E. Lopez-Calle, P. Espindola, C. Boehm, T. Brueckner, J. Spinke, M. Marcinowski, T. Keller, A. Tgetgel, N. Herbert, T. Fischer and E. Beiersdorf, *Analyst*, 2017, **142**, 4206–4214.
304 M. Shen, N. Li, Y. Lu, J. Cheng and Y. Xu, *Lab Chip*, 2020, **20**, 2626–2634.
305 M. Geissler, L. Clime, X. D. Hoa, K. J. Morton, H. Hébert, L. Poncelet, M. Mounier, M. Deschênes, M. E. Gauthier, G. Huszczynski, N. Corneau, B. W. Blais and T. Veres, *Anal. Chem.*, 2015, **87**, 10565–10572.
306 L. M. Dignan, M. S. Woolf, J. A. Ross, C. Baehr, C. P. Holstege, M. Pravetoni and J. P. Landers, *Anal. Chem.*, 2021, **93**, 16213–16221.
307 S. Okamoto and Y. Ukita, *Sens. Actuators, B*, 2018, **261**, 264–270.
308 R. D. Johnson, I. H. A. Badr, G. Barrett, S. Lai, Y. Lu, M. J. Madou and L. G. Bachas, *Anal. Chem.*, 2001, **73**, 3940–3946.
309 S. Li, Z. Ma, Z. Cao, L. Pan and Y. Shi, *Small*, 2020, **16**, 1903822.
310 S. Pagliara, A. Camposeo, A. Polini, R. Cingolani and D. Pisignano, *Lab Chip*, 2009, **9**, 2851.

 This journal is © The Royal Society of Chemistry 2023

Open Access Article. Published on 26 June 2023. Downloaded on 10/28/2025 9:16:10 PM.
This article is licensed under a Creative Commons Attribution 3.0 Unported Licence.

311 P. N. Floriano, N. Christodoulides, D. Romanovicz, B. Bernard, G. W. Simmons, M. Cavell and J. T. McDevitt, *Biosens. Bioelectron.*, 2005, **20**, 2079–2088.
312 R. Lanfranco, J. Saez, E. Di Nicolò, F. Benito-Lopez and M. Buscaglia, *Sens. Actuators, B*, 2018, **257**, 924–930.
313 A. K. Ellerbee, S. T. Phillips, A. C. Siegel, K. A. Mirica, A. W. Martinez, P. Striehl, N. Jain, M. Prentiss and G. M. Whitesides, *Anal. Chem.*, 2009, **81**, 8447–8452.
314 M. S. Wiederoder, L. Peterken, A. X. Lu, O. D. Rahmanian, S. R. Raghavan and D. L. DeVoe, *Analyst*, 2015, **140**, 5724–5731.
315 I. Moser, *Biosens. Bioelectron.*, 2002, **17**, 297–302.
316 H. Muñoz-Galán, C. Alemán and M. M. Pérez-Madrigal, *Lab Chip*, 2023, **23**, 1128–1150.
317 N. Krakover, R. Ilic and S. Krylov, in *2018 IEEE Micro Electro Mechanical Systems (MEMS)*, 2018, pp. 846–849.
318 T.-V. Nguyen, Y. Mizuki, T. Tsukagoshi, T. Takahata, M. Ichiki and I. Shimoyama, *Sensors*, 2020, **20**, 1052.
319 R. Zhang, Q. Li, L. Tian, J. Gong, Z. Li, W. Liu and L. Gui, *J. Micromech. Microeng.*, 2021, **31**, 055013.
320 C.-H. Lin, C.-K. Wang, Y.-A. Chen, C.-C. Peng, W.-H. Liao and Y.-C. Tung, *Sci. Rep.*, 2016, **6**, 36425.
321 X. Lin, X. Huang, K. Urmann, X. Xie and M. R. Hoffmann, *ACS Sens.*, 2019, **4**, 242–249.
322 K. Shah, W. C. Shin and R. S. Besser, *Sens. Actuators, B*, 2004, **97**, 157–167.
323 S. V. Karnik, M. K. Hatalis and M. V. Kothare, *J. Microelectromech. Syst.*, 2003, **12**, 93–100.
324 M. Polino, H. S. Rho, M. P. Pina, R. Mallada, A. L. Carvalho, M. J. Romão, I. Coelhoso, J. G. E. Gardeniers, J. G. Crespo and C. A. M. Portugal, *Membranes*, 2021, **11**, 549.
325 G. K. Batchelor, *An Introduction to Fluid Dynamics*, Cambridge University Press, Cambridge, 2000.